CHAPTER ONE
INTRODUCTION

1.1 General Concept

With increased penetration of wind generation into power systems over the years, there are requirements for power sources to contribute to network support rather than being disconnected from the network then abnormal grid voltage is detected. For wind farms connected with long transmission lines to the ac grid, voltage unbalance may arise due to a number of reasons, such as asymmetric line impedances and loads. The unbalanced voltage can have a significant effect on the performance and stability of connected equipment (e.g. induction machines). Most early wind farms use wind turbines based on the fixed-speed induction generator (FSIG) whereas many recent wind farms use doubly-fed induction generator (DFIG) based wind turbines [1].

In order to meet power needs, taking into account economical and environmental factors, wind energy conversion is gradually gaining interest as a suitable source of renewable energy. The electromagnetic conversion is usually achieved by induction machines or synchronous and permanent magnet generators. Squirrel cage induction generators are widely used because of their lower cost, reliability, construction and simplicity of maintenance. But when it is directly connected to a power network, which imposes the frequency, the speed must be set to a constant value by a mechanical device on the wind turbine. Then, for a high value of wind speed, the totality of the theoretical power can be extracted. To overcome this problem, a converter, which must be dimensioned for the totality of the power exchanged, can be placed between the stator and the network. In order to enable variable speed operations with a lower rated power converter, double-fed induction generator (DFIG) can be used. The stator is directly connected to the grid and the rotor is fed to magnetize the machine [2].

For a wind farm to be connected to the network it must comply with standards specified in the relevant grid code. One area of particular concern is fault ride-through. Studies have shown that FSIG based wind farms have difficulties in meeting the requirements for fault ride-through without dynamic reactive power compensation [3].

The conventional energy sources are limited and have pollution to the environment. So more attention and interest have been paid to the utilization of renewable energy sources such as wind energy, fuel cell and solar energy etc. Wind energy is the fastest growing and most promising renewable energy source among them due to economical viable. Doubly-fed induction machines are receiving increasing attention for wind energy conversion system during such situation. Because the main advantages of such machines is that, if the rotor current is governed applying field orientation control-carried out using commercial double sided PWM inverter, decoupled control of stator side active and reactive power results and the power processed by the power convertor is only a small fraction of the total system power [4].

Some methods of conventional power production shall be replaced in the future by improving the efficiency of electricity use, conversion to renewable forms of energy and other environmentally acceptable electricity production technologies. One of the solutions in this case is the wind power use [5].

There are two basic types of wind turbines used nowadays

- Fixed-speed wind turbines
- Variable-speed wind turbines

Fixed-speed wind turbines are mainly equipped with squirrel-cage induction generators, which are also known as self-excited generators. Self-excited generators work within a limited wind speed range, which is one of their main drawbacks in comparison with variable-speed wind turbines. They can be manufactured as one- or two-speed versions and they are suitable for low power ranges up to 2 MW. The majority of modern megawatt wind turbines are variable-speed wind turbines

equipped with a Doubly Fed Induction Generator (DFIG) that is coupled to the power grid via a main transformer and supplied to the rotor from a frequency convertor. The main advantage of DFIG wind turbines is their ability to supply power at a constant voltage and frequency while the rotor speed varies. The DFIG concept of a variable-speed wind turbine also makes possible the controlling of the active and reactive power, which is a significant advantage as regards grid integration [6].

The doubly fed induction generator (DFIG) can supply power at constant voltage and constant frequency while the rotor speed varies. This makes it suitable for variable speed wind energy application. Additionally, when a bidirectional AC-AC converter is used in the rotor circuit, the speed range can be extended above synchronous speed and power can be generated both from the stator and the rotor. An advantage of this type of DFIG drive is that the rotor converter need only be rated for a fraction of the total output power, the fraction depending on the allowable sub- and super-synchronous speed range [7].

Figure (1.1) shows the general concept of the doubly-fed induction generator. The mechanical power generated by the wind turbine is transformed into electrical power by an induction generator and is fed into the main grid through the stator and the rotor windings. The rotor winding is connected to the main grid by self commutated AC/DC converters allowing controlling the slip ring voltage of the induction machine in magnitude and phase angle. In contrast to a conventional, singly-fed induction generator, the electrical power of a doubly-fed induction machine is independent from the speed. Therefore, it is possible to realize a variable speed wind generator allowing adjusting the mechanical speed to the wind speed and hence operating the turbine at the aerodynamically optimal point for a certain wind speed range [8].

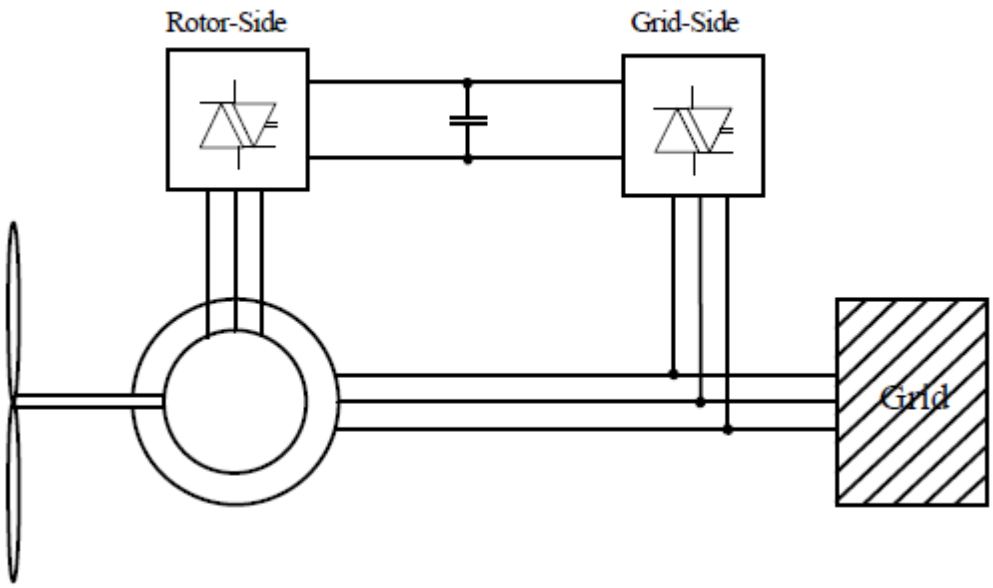

Figure 1.1 Doubly-fed induction generator system

1.2 Motivations

To improve wind generation system efficiency and power quality, adjustable speed wind generators are used to track maximum wind power output and to control the system more flexible, therefore doubly-fed induction generators are developed and applied widely in the large wind generation system. While most conventional wind farms were based on fixed speed induction generators (FSIG), more recent instilments tend to use the doubly-fed induction generators (DFIG). DFIGs offer several advantages when compared with FSIGs. These advantages, including speed control, reduced flicker, and four-quadrant active and reactive power capabilities, are primarily achieved via control of the rotor side converter (RSC), which is typically rated at 30% of the generator rating for a given rotor speed operating range of 0.75-1.25 pu [3].

Doubly fed induction generator (DFIGs) are widely used in modern wind turbines due to their full power control capability, variable speed operation, low converter cost, and reduced power loss compared to other solutions such as fixed speed

induction generators or fully rated converter system [9]. Doubly fed induction generators can also contribute to reduced network unbalance due to its control flexibility.

1.3 The Research Objectives

- To understanding the doubly-fed induction generators.
- Study the operating characteristics of the DFIG.
- Develop and discuss a dynamic model of the DFIG used in wind turbine.
- To develop a control strategy to control real and reactive power from a generator to ensure maximum output power and voltage stability.
- Simulation analysis is performed to investigate a variety of DFIG characteristics.

1.4 Problem Statement

Analysis of the Doubly-Fed Induction Generator (DFIG) for Wind Turbines application both during steady-state operation and transient operation .In order to analyze the DFIG during transient operation both the control and modeling of the system is of importance. Hence, the control and the modeling are also important parts of the thesis. The main contribution of this thesis is dynamic and steady-state analysis of the doubly-fed induction generators.

1.5 Methodology

The steady state characteristics of a Wind energy conversion system using doubly fed induction generator (DFIG) are analyzed using MATLAB. The dynamic steady-state simulation model of the DFIG is developed using MATLAB. Simulation analysis is performed to investigate a variety of DFIG characteristics, including torque-speed, real and reactive-power over speed characteristics. Based on the analysis, the DFIG operating characteristics are studied.

1.6 Thesis layout

This dissertation consists of five chapters. The literature review of doubly fed induction generators modeling, control and DFIG in wind turbine are introduced in

chapter two. The mathematical models of doubly fed induction generators and control are presented in chapter three. Chapter four presents the simulation results and discussion. Finally, chapter five draws the conclusions, recommendations for future research and author's contribution.

CHAPTER TWO
LITERATURE REVIEW

2.1 Introduction

Renewable energy including solar, wind, tidal, small hydro geothermal, refused derived fuel cell energies is sustainable, reusable and environment-ally friendly and clean. With the increasing shortage in fossil fuels, and pollution problems renewable energy has become an important energy source. Among the other renewable energy sources wind energy has proven to be one of the most economical one. Earlier constant speed wind energy conversion systems (WECS) were proposed to generate constant frequency voltages from the variable wind. However, Variable speed wind energy conversion system operations can be considered advantageous, because additional energy can be collected as the wind speed increases. Variable speed WECS must use a power electronic converter. They are classified as full power handling WECS and partial power handling WECS. In full power handling WECS, the power converter is in series with the induction or synchronous generator, in order to transform the variable amplitude/frequency voltages into constant amplitude/frequency voltages and the converter must handle the full power. In a partial power handling WECS, the converter processes only a portion of the total generated power (eg slip power) which poses an advantage in terms of the reduced cost converter of the system and increased efficiency of the system [11].

Due to the energy crisis, alternative renewable resources have assumed increased importance leading to relevant technological efforts. Wind energy has been identified as an affordable promising resource for such exploitation. The wind energy conversion system safely and efficiently turns wind into electrical energy. It is predicated that nearly 10% of the world energy needs could be met by the wind energy by the year 2020 [12].

In the 1990s, wind power turbines were characterized by a fixed-speed operation. Basically, they consisted of the coupling of a wind turbine, a gearbox and an induction machine directly connected to the grid. Additionally, they used a soft starter to energize the machine and a bank of capacitor to compensate the machine power reactive absorption. Although being simple, reliable and robust, the fixed-speed wind turbines were inefficient and power fluctuations were transmitted to the network due to wind fluctuations. In the mid- 1990s, variable-speed wind power turbines gave an impulse to the wind power industry. A better turbine control reduces power fluctuations. In addition, optimal power extraction from wind was possible by operating the turbine at optimal speed. Among the different configurations of variable-speed wind power turbine, the doubly-fed induction generator, at present, is the most used in the development of wind farm projects. This configuration consists of the coupling of a turbine, a gearbox and an induction machine doubly connected to the grid directly connected from the stator circuits and indirectly connected from the rotor circuits by using converters [13].

2.2 Wind Turbine System

Wind turbines system (WTS) can either operate at fixed speed or variable speed. For a fixed speed wind turbine the generator is directly connected to the electrical grid. For a variable speed wind turbine the generator is controlled by power electronic equipment. There are several reasons for using variable-speed operation of wind turbines; among those are possibilities to reduce stresses of the mechanical structure, acoustic noise reduction and the possibility to control active and reactive power [5],[10].

Most of the major wind turbine manufactures are developing new larger wind turbines in the 3-to-5 MW range. These large wind turbines are all based on variable speed operation with pitch control using a direct driven synchronous generator (without gearbox) or a doubly-fed induction generator (DFIG). Fixed-speed induction generators with stall control are regarded as unfeasible for this large wind

turbine. Today, doubly-fed induction generators are commonly used by the wind turbine industry for larger wind turbines [5],[10].

The power electronic equipment makes it possible to control the rotor speed. In this way the power fluctuation caused by wind variations can be more or less absorbed by changing the rotor speed and thus power variation originating from the wind conversion and the drive train can be reduced. Hence the power quality impact caused by the wind turbine can be improved compared to a fixed-speed turbine.

The rotational speed of a wind turbine is fairly low and must therefore be adjusted to the electrical frequency. This can be done in two ways: with a gearbox or with the number of pole pairs of the generator. The number of pole pairs sets the mechanical speed of the generator with respect to the electrical frequency and the gearbox adjusts the rotor speed of the turbine to the mechanical speed of the generator [12].

Variable-speed turbines have many advantages in comparison with constant-speed turbines. Variable-speed improves the dynamic behavior of the turbine, increases the power production and reduces noise at low wind speed. In addition, by using a voltage source converter for the variable-speed system, grid currents can be controlled to be sinusoidal without low-frequency harmonics and the reactive power can be chosen freely [12].

2.3 Doubly-Fed Induction Generator System For Wind Turbines

For variable-speed systems with limited variable-speed range, e.g.±30% of synchronous speed, the DFIG can be an interesting solution. As mentioned earlier the reasons for this are that power electronic convertor only has to handle a fraction (20-30%) of total power. This means that the losses in power electronic converter can be reduced compared to a system where the converter has to handle the total power. In addition, the cost of the converter becomes lower. The stator circuit of the DFIG is connected to the grid while the rotor circuit is connected to a convertor via slip ring, see Figure 2.1[10].

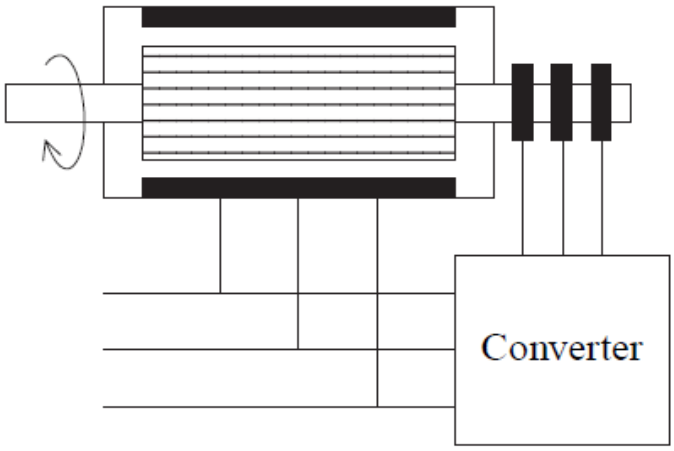

Figure 2.1 Principle of the doubly-fed induction generator

A more detailed picture of the DFIG system with a back-to-back converter can be seen in Figure 2.2 [5],[10]. The back-to-back convertors consist of two convertors, i.e. machine side and grid side convertor that are connected back-to-back. Between the two convertors a dc-link capacitor is placed, as energy storage, in order to keep the voltage variation (or ripple) in the dc-link voltage small.

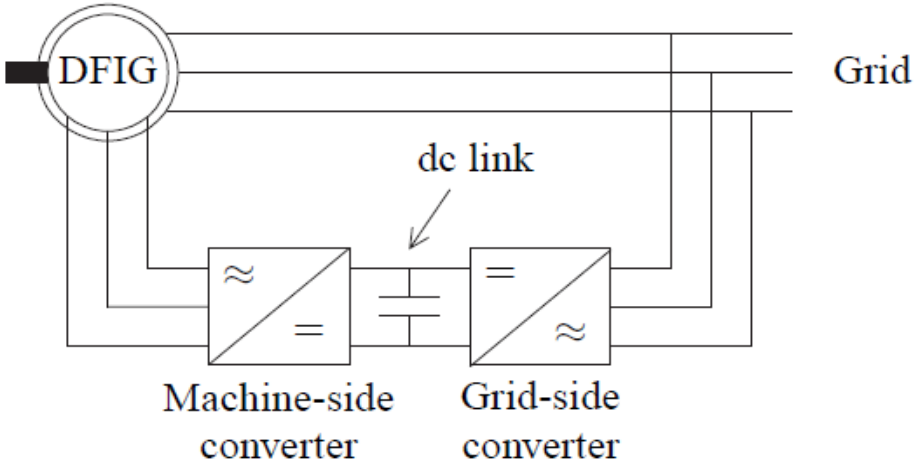

Figure 2.2 DFIG systems with a back-to-back convertor

With the machine side convertor it is possible to control the torque or the speed of the DFIG and also the power factor at the stator terminals, while the main objective for the grid side convertor is to keep the dc-link voltage constant [5],[10].

2.4 Types of Doubly-Fed Induction Machines

In this section a short presentation of other kinds of doubly-fed induction machines is made: a cascaded doubly-fed induction machines, a single-frame cascaded doubly-fed induction machines, a brushless doubly-fed induction machines and doubly-fed reluctance machine.

2.4.1 Cascaded Doubly-Fed Induction Machine

The cascaded doubly-fed induction machine consists of two doubly-fed induction machines with wound rotors that are connected mechanically through the rotor and electrically through the rotor circuits. The stator circuit one of the machines is directly connected to the grid whiles the other machines stator is connected via a convertor to the grid. Since the rotor voltages of both machines are equal, it is possible to control the induction machine that is directly connected to the grid with the other induction machine.

2.4.2 Single-Frame Cascaded Doubly-Fed Induction Machine

The single-frame cascaded doubly-fed induction machine is a cascaded doubly-fed induction machine, but with the two induction machines in one common frame. Although this machine is mechanically more robust than cascaded doubly-fed induction machine, it suffers from comparative low efficiency.

2.4.3 Brushless Doubly-Fed Induction Machine

This is an induction machine with two stator windings in the same slot. That is, one winding for the power and one winding for the control. To avoid a direct transformer coupling between the two-stator windings, they cannot have the same number of pole pairs. Furthermore, to avoid unbalanced magnetic pull on the rotor the difference between the pole pairs must be great than one. The number of poles in the rotor must equal the sum of the number of poles in the two stator winding.

2.4.4 Doubly-Fed Reluctance Machine

The stator of the doubly-fed reluctance machine is identical to the brushless doubly-fed induction machine, while the rotor is based on the principle of reluctance [10].

2.5 Doubly-Fed Induction Machines In Wind Turbine

Wind energy is popular renewable energy source. Doubly-fed induction generator (DFIG) wind turbines are used widely by all the wind generator manufactures. In Figure 2.3 a basic layout of DFIG wind turbine system is shown. The rotor circuit is connected through slip rings to the back to back convertors arrangement controlled by PWM strategies.

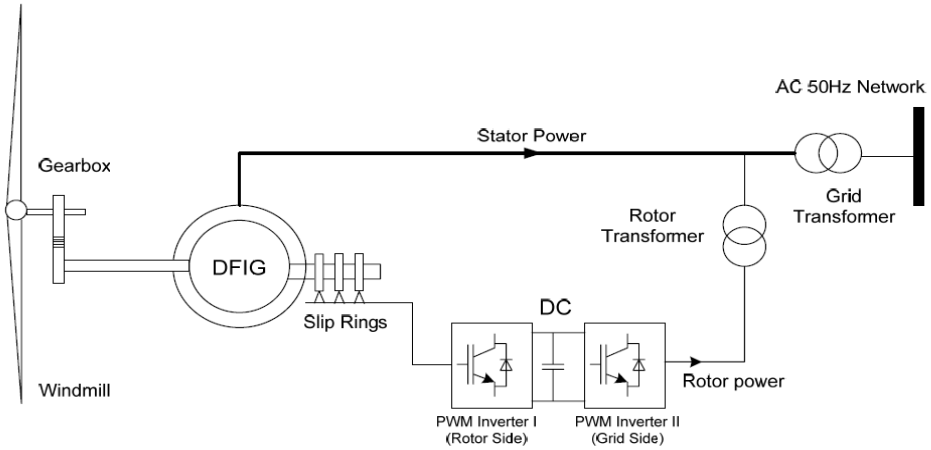

Figure 2.3 DFIG wind turbine system

2.6 Doubly-Fed Induction Generator Control

Doubly fed induction generator system have two major control areas: electrical control of the convertors and mechanical control of the blade pitch angle. Control of the DFIG is more complicated than the control of a standard induction machines. In order to control the DFIG the rotor current is controlled by a power electronic convertor. One common way of controlling the rotor current is by means of field-oriented (vector) control. One common way is to control the rotor current with stator-flux orientation, or with air-gap flux orientation. If the stator resistance can be considered small, stator-flux orientation gives in principle orientation also with the stator voltage (grid-flux orientation) [5],[10].

Traditionally, the DFIG is controlled using vector control (VC), which decouples the rotor currents into active power (or torque) and reactive power (or flux) components and adjusts them separately in a reference frame fixed to either the stator flux or voltage. Current controllers are then utilized to regulate the rotor currents. The main drawback for VC is its linear nature which does not consider the discrete operation of power electronics converters. Thus, in order to maintain system stability over the whole operation range and adequate dynamic response under both normal and abnormal conditions, the current controller and its control parameters must be carefully turned [9],[14].

The rotor side converter is used to provide speed/stator output active power control, along with terminal voltage and reactive power control, by decoupling the rotor current into real and imaginary parts, using stator flux oriented vector control. The real current component reference is taken from an optimal power tracking current, which allows the generator to produce maximum power for a given wind speed [15].

2.7 Summary

A wind energy conversion system (WECS) differs from a conventional power system. The power output of a conventional power plant can be controlled whereas the power output of a (WECS) depends on the wind. The doubly-fed induction generator used as a wind turbine generator has recently received a great attention from the industrial and scientific communities. The reason is twofold: first, this machine easily produces a fixed frequency voltage from the stator winding when the rotor is driven at variable speed; second: the excitation power electronic convertor feeding the rotor windings needs to be rated at a fraction of the nominal power of the generator. Consequently, this machine is often the natural choice for electricity generation from renewable energy sources.

CHAPTER THREE
MATHEMATICAL MODEL OF DFIG AND CONTROL

3.1 Introduction

The Induction Machine can be represented by the transformer per phase equivalent circuit model where R_r and X_r represent rotor resistance and reactance referred to the stator side. The primary internal stator induced voltage E_{si} is coupled to the secondary rotor induced voltage E_r by an ideal transformer with an effective turn ratio a_{eff}. But the equivalent circuit of Figure 3.1 differs from the transformer equivalent circuit primarily in the effects of varying rotor frequency on the rotor voltage E_r [11].

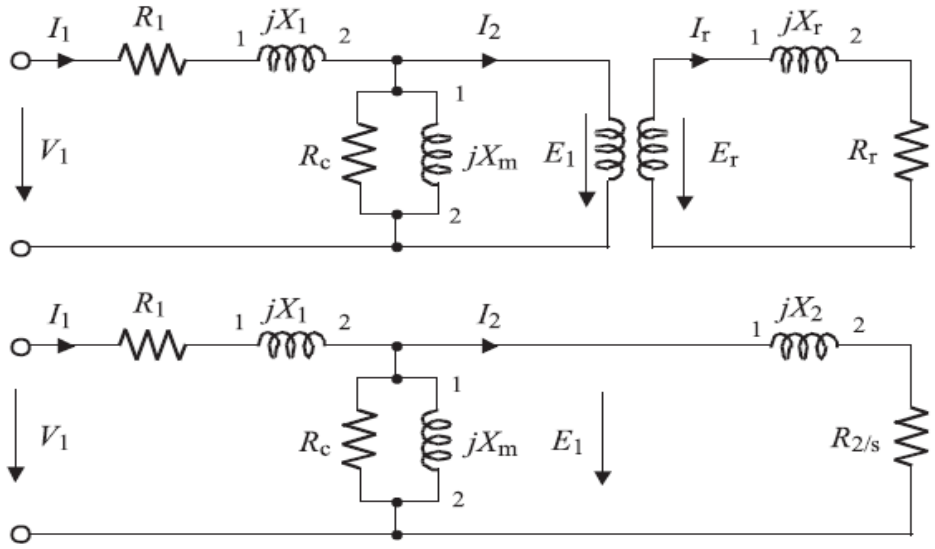

Figure 3.1 Conventional induction machine equivalent circuit

In the case of doubly-fed induction machines, however there is a voltage injected in to the rotor windings so that the normal induction machine equivalent circuit of Figure 3.1 needs to be modified by adding a rotor injected voltage as shown in Figure 3.2 [11].

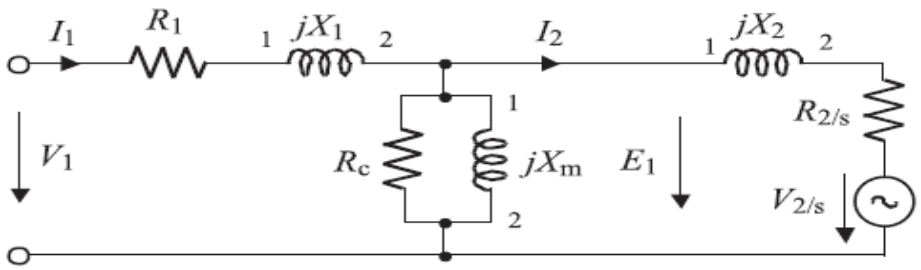

Figure 3.2 Equivalent circuit of DFIG

From the equivalent circuit, for a doubly-fed induction machine the real and reactive power of stator P_{sw}, P_{sQ} and rotor P_{rw}, P_{rQ} can be derived as follows:

$$P_{SW} = 3V_1 I_1 \cos(\Phi_{v1} - \Phi_{i1}) \quad (3.1)$$
$$P_{SQ} = 3V_1 I_1 \sin(\Phi_{v1} - \Phi_{i1}) \quad (3.2)$$
$$P_{rw} = 3V_2 I_2 \cos(\Phi_{v2} - \Phi_{i2}) \quad (3.3)$$
$$P_{rQ} = 3V_2 I_2 \sin(\Phi_{v2} - \Phi_{i2}) \quad (3.4)$$

As mentioned earlier the DFIG system consist of a DFIG and back-to-back voltage source converter with a dc link. The back-to-back converters consist of a grid-side converter (GSC) and machine side converter (MSC) [10].

3.2 DFIG Model

Due to its simplicity for deriving control laws for the DFIG, the T representation of the induction generator model will be used. Note, that from a dynamic point of view, the rotor and the stator leakage inductance have the same effect. Therefore, it is possible to use a different representation of the park model in which the leakage inductance is placed in the rotor circuit, the so-called *T* representation of the induction machine. The name is due to the formation of a *"T"* of the inductances see Figure 3.3 [10].

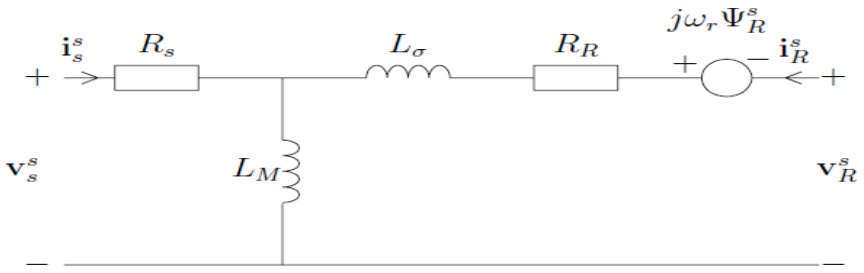

Figure 3.3 T representation of the Induction Generator

This model is described by the following space-vector equations in stator:

$$V_s^s = R_s I_s^s + \frac{d\Psi_s^s}{dt} \tag{3.5}$$

$$V_R^s = R_R I_R^s + \frac{d\Psi_R^s}{dt} - j\omega\Psi_R^s \tag{3.6}$$

Where superscript s indicates stator coordinates. The model can also be described in synchronous coordinates as:

$$V_S = R_S I_S + \frac{d\Psi_S}{dt} + j\omega_1 \Psi_S \tag{3.7}$$

$$V_R = R_R I_R + \frac{d\Psi_R}{dt} + j\omega_2 \Psi_R \tag{3.8}$$

Where the following notation is used:

$V_s \Rightarrow$ Stator voltage	$\Psi_s \Rightarrow$ Stator flux
$V_R \Rightarrow$ Rotor voltage	$\Psi_R \Rightarrow$ Rotor flux
$I_s \Rightarrow$ Stator current	$R_s \Rightarrow$ Stator resistance
$I_R \Rightarrow$ Rotor current	$R_R \Rightarrow$ Rotor resistance
$\omega_1 \Rightarrow$ Synchronous frequency	$\omega_2 \Rightarrow$ Slip frequency

The stator flux, rotor flux and electromechanical torque are given by:

$$\Psi_s = L_M(i_s + i_R) \tag{3.9}$$

$$\Psi_R = (L_M + L_\sigma)i_R + L_M i_s = \Psi_s + L_\sigma i_R \tag{3.10}$$

$$T_e = 3npI_m[\Psi_s i_R^*] \tag{3.11}$$

Where L_M is the magnetizing inductance, $L\sigma$ is the leakage inductance and *np* is the number of pole pairs. Finally, the mechanical dynamics of the induction machine are described by:

$$\frac{J}{np}\frac{d\omega_r}{dt} = T_e - T_s \tag{3.12}$$

Where *J* is the inertia and T_s is the shaft torque [10].

3.2.1 Grid-Filter Model

In the Figure 3.4 the equivalent circuit of the grid filter in stator coordinates can be seen. The filter consist of an inductance L_f and its resistance R_f. Applying Kirchhoff's voltage law to the circuit in the figure the following model in synchronous coordinates can be found:

$$E_g = -\left(R_f + j\omega_1 L_f\right) i_f - L_f \frac{di_f}{dt} + V_f \tag{3.13}$$

Where E_g is the grid voltage, i_f is the grid-filter current, and V_f is the grid-filter voltage supplied from the grid-side converter [10].

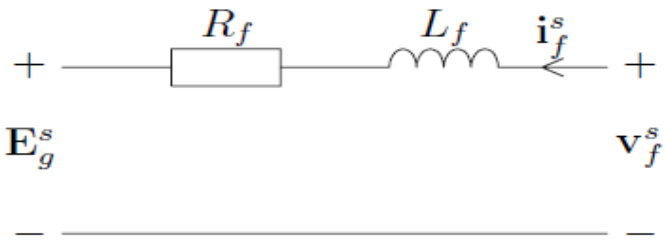

Figure 3.4 Grid-filter model in stator coordinates

3.2.2 DC-Link Model

The energy, W_{dc} stored in the dc-link capacitor, C_{dc} is given by

$$W_{dc} = \frac{1}{2} C_{dc} V_{dc}^2 \tag{3.14}$$

Where V_{dc} is the dc-link voltage, In Figure 3.5 an equivalent circuit of the dc-link model, where the definition of the power flow through the grid-side converter (GSC) and the machine-side converter (MSC), can be seen. Moreover if the losses in the actual converter can be considered small and thereby be neglected, the energy in the dc-link capacitor is dependent on the power delivered to the grid filter, P_f and the power delivered to the rotor circuit of the DFIG P_r [10].

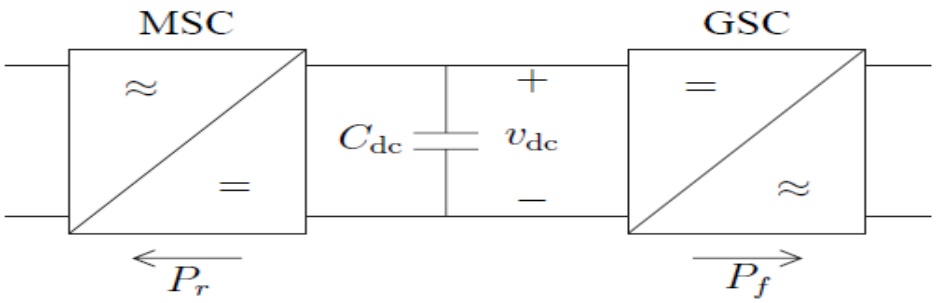

Figure 3.5 DC-Link Model

$$\frac{dW_{dc}}{dt} = \frac{1}{2} C_{dc} \frac{d}{dt} V_{dc}^2 = -P_f - P_r \quad (3.15)$$

This means that the dc-link voltage will vary as

$$C_{dc} V_{dc} \frac{dV_{dc}}{dt} = -P_f - P_r \quad (3.16)$$

This means that $P_f = P_r$ for a constant dc-link voltage.

The total model of the DFIG system presented in Figure 3.6 and can be summarized in synchronous coordinate, as

$$\frac{d\Psi_s}{dt} = E_g - R_s i_s - j\omega_1 \Psi_s \quad (3.17)$$

$$\frac{d\Psi_R}{dt} = V_R - R_R i_R - j\omega_2 \Psi_R \quad (3.18)$$

$$L_f \frac{di_f}{dt} = V_f - \left(R_f + j\omega_1 L_f\right) i_f - E_g \quad (3.19)$$

$$C_{dc} V_{dc} \frac{dV_{dc}}{dt} = -P_f - P_r \quad (3.20)$$

$$\frac{J}{np} \frac{d\omega_r}{dt} = T_e - T_s \quad (3.21)$$

Where:

$$\Psi_s = L_M (i_s + i_R) \quad (3.22)$$

$$\Psi_R = L_\sigma i_R + L_M (i_s + i_R) \quad (3.23)$$

$$T_e = 3npI_m [\Psi_s i_R^*] \quad (3.24)$$

$$P_r = 3R_e [V_R i_R^*] \quad (3.25)$$

$$P_f = 3R_e \left[V_f i_f^*\right] \quad (3.26)$$

Note that in (3.17) that the stator voltage, *Vs*, has been changed to the grid voltage, E_g [10].

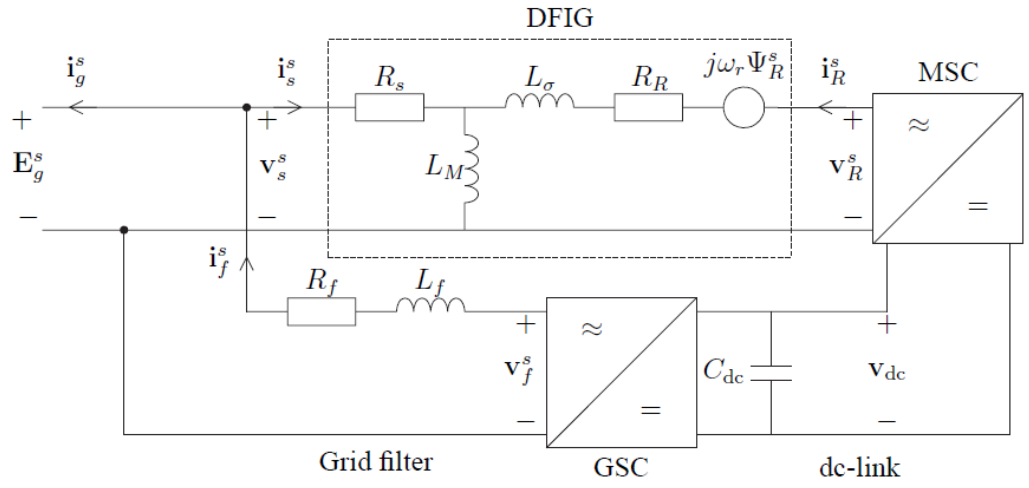

Figure 3.6 Equivalent circuit of the DFIG system

3.3 Control of DFIG

The control system consists of two controllers. One controller is a speed controller which is used to control the torque of generator to make the wind turbine absorb the maximum power from the wind when wind speed is under rated speed. The feed-forward compensator and loop shaping are used for this controller design. The design of the speed controller is easy and has better robustness than PI controller. The other is a pitch controller that it used to regulate the pitch angle of the blade. Considering the grate mechanical inertia of the blade, we set five given pitch-angles in this controller. This can simplify the design of pitch controller and is easy to implement in practice [16].

The phase sequence of the AC voltage generated by the rotor side converter is positive for sub synchronous speed and negative for super synchronous speed. The frequency of this voltage is equal to the product of the grid frequency and the absolute value of the slip. The rotor side and the grid side converter have the capability of generating or absorbing reactive power and could be used to control the reactive power or the voltage at the grid terminals. The rotor side converter is used

to control the wind turbine output power and the voltage (reactive power) measured at the grid terminals. The grid side converter is used to regulate the voltage of the DC bus capacitor [11].

Different strategies were proposed in the literature to solve the DFIG control problem. A vector controlled doubly-fed induction generator is an attractive solution for high performance restricted speed-range electric drives and energy generation application [17][18].

In order to control the rotor current of a DFIG by means of vector control, the reference frame has to be aligned with a flux linkage. One common way is to control the rotor currents with stator-flux orientation, or with air-gap-flux orientation. If the stator resistance is considered to be small, stator-flux orientation gives orientation also with the stator voltage [10].

3.4 Control of Machine-Side Converter

The main task of the machine-side converter is, of course, to control the machine. This is done by having an inner fast field-oriented current control loop that controls the rotor current. The field orientation could, for example, either be aligned with the stator flux of the DFIG or the grid flux. For both reference frames the q component of the rotor current largely determines the produced torque while the d component can be used to control for instance, the reactive power at the stator terminals [10].

3.4.1 Current Control

As mentioned earlier, it is common to control the rotor current with either stator-flux orientation or grid-flux orientation. In order to derive the rotor-current control law, it is advantageous i_s and Ψ_R from (3.7) and (3.8) which yields

$$V_s = -R_s i_R + \frac{d\Psi_s}{dt} + \left(\frac{R_s}{L_M} + j\omega_1\right)\Psi_s \tag{3.27}$$

$$V_R = (R_R + j\omega_2 L_\sigma) i_R + L_\sigma \frac{di_R}{dt} + \frac{d\Psi_s}{dt} + j\omega_2 \Psi_s$$

$$= (R_R + R_s + j\omega_2 L_\sigma) i_R + L_\sigma \frac{di_R}{dt} + E \tag{3.28}$$

$$E = V_s - \left(\frac{R_s}{L_M} + j\omega_r\right)\Psi_s \tag{3.29}$$

Where E is the back EMF, the rotor current dynamics formed by the inner loop in Figure 3.7 bellow

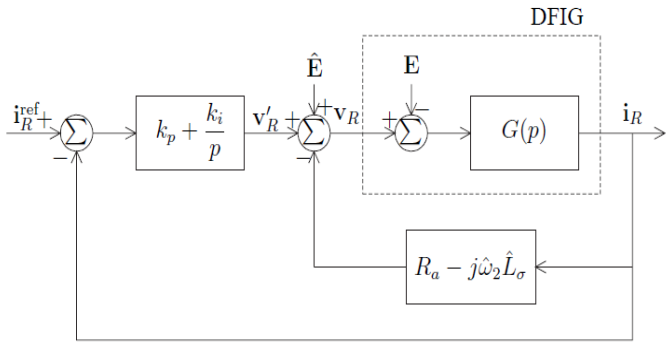

Figure 3.7 Block diagram of the current control system

3.4.2 Torque Control

The electromechanical torque can be found from (3.11) as

$$T_e = 3npI_m[\Psi_s i_R^*] \approx -3np\Psi_s i_{Rq} \tag{3.30}$$

For a stator-flux-oriented system the above approximation is actually equality. Since the stator flux, Ψ_s is almost fixed to the stator voltage; the torque can be controlled by the q component of the rotor current, i_{Rq}. Since it is difficult to measure the torque, it is most often controlled in an open-loop manner. Therefore the q component reference current, i_{Rq}^{ref}, can be determined from the reference torque T_e^{ref} as [4].

$$i_{Rq}^{ref} = -\frac{T_e^{ref}}{3np\,\Psi_s} \tag{3.31}$$

Fig.(3-8) shows a block diagram of the open-loop torque control scheme.

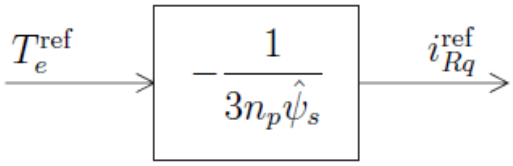

Figure 3.8 Block diagram of the open-loop torque control

3.4.3 Speed Control

Since the current dynamics, that is, with the band width α_c should be set much faster than the speed dynamics, the speed can be controlled in cascade with the current. The mechanical dynamics are described by

$$\frac{J}{np}\frac{d\omega_r}{dt} = T_e - T_s \tag{3.32}$$

Where T_e is the electromechanical torque and T_s is the shaft torque. The electromechanical torque can be expressed, under the assumption that the current dynamics are much faster than the speed dynamics, as

$$T_e = T_e^{ref} \tag{3.33}$$

Where the reference torque is set to

$$T_e^{ref} = T'^{ref}_e - B_a\omega_r \tag{3.34}$$

The Figure 3.9 shows a block diagram of the speed control system [10].

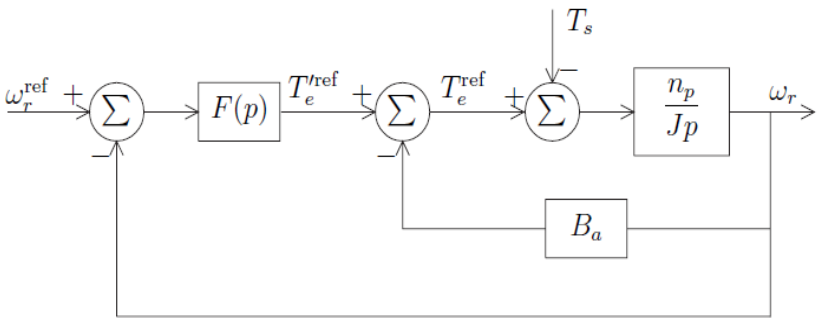

Figure 3.9 Speed control loop

3.5 Control of Grid-Side Converter

The main objective of the grid-side converter is to control the dc-link voltage. The control of the grid-side converter consists of a fast inner current control loop, which controls the current through the grid filter, and an outer slower control loop that controls the dc-link voltage. The reference frame of the inner current control loop will be aligned with the grid flux. This means that the q component of the grid filter current will control the active power delivered from the converter and the d

component of the filter current will, accordingly, control the reactive power. This implies that the outer dc-link voltage control loop has to act on the q component of the grid-filter current [10].

3.5.1 Current Control of Grid Filter

In (3.19) the dynamic of the grid filter are described

$$L_f \frac{di_f}{dt} = V_f - \left(R_f + j\omega_1 L_f\right) i_f - E_g \tag{3.35}$$

In order to introduce "active damping" and decouple the d and the q components of the grid-filter current, the applied grid-filter voltage, V_f is chosen as

$$V_f = V'_f - \left(R_{af} - j\omega_1 L_f\right) i_f \tag{3.36}$$

This means that the inner closed-loop transfer function, assuming ideal parameters, becomes

$$G(p) = \frac{i_f(p)}{V'_f(p)} = \frac{1}{L_{fp} + R_f + R_{af}} \tag{3.37}$$

3.5.2 DC-Link Voltage Control

One way of simplifying the control of the dc-link voltage is by utilizing feedback linearization, i.e. the nonlinear dynamics of the dc-link are transformed into an equivalent linear system where linear control techniques can be applied. A block diagram of the dc-link voltage controller is depicted in Figure 3-10 [10].

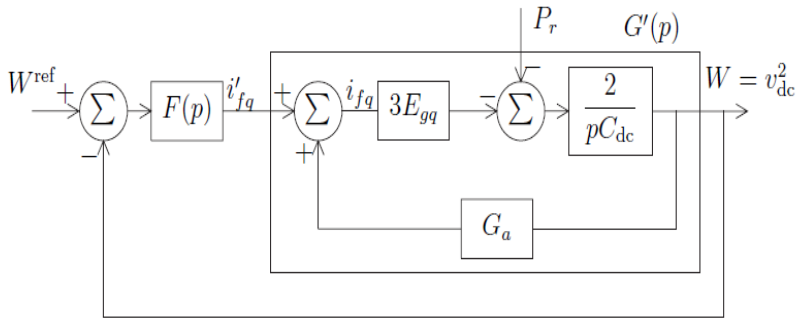

Figure 3.10 Dc-link voltage control loop

3.6 Summary

Mathematical modeling of converter system is realized by using various types of models, which can be broadly divided into two groups: mathematical functional models and mathematical physical models. Owing to the fact that DFIG controls have a significant influence on the system dynamics, vector control is applied for both stator and rotor side converters to increase the degree of controllability, where fixed-frequency internal model controller approach is adopted to design the controllers precisely.

CHAPTER FOUR
RESULTS AND DISCUSSIONS

4.1 Introduction

Large Wind turbines are often equipped with doubly-fed induction generators. There are several advantages by using adjustable speed generators. Modern wind turbines use complex technologies including power electronic converters and sophisticates control systems. Electromagnetic transients need to be simulated and analyzed in order to study the impact of these generators on the power systems. Methods and tools for simulation of wind turbines in large power systems are therefore needed [19].

In this dissertation a detailed model from Matlab & Simulink SimPower systems library is used. The detailed model includes detailed representation of power electronic IGBT, the model must be discredited at a relatively small time step (5 microsecond). This model is well suited for observing harmonics and control systems dynamic performance over relatively short periods of times (typically hundreds of milliseconds to one second) [20].

4.2 Circuit Description

A 9 MW wind farm consisting of six 1.5 MW wind turbines connected to a 25 KV distribution system exports power to a 120 KV grid through a 30 Km, 25 KV feeder, as shown in Figure 4.1 below

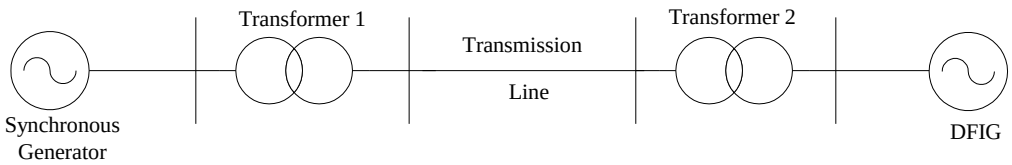

Figure 4.1 detailed model of DFIG

Wind turbines using a doubly-fed induction generator (DFIG) consist of a wound rotor induction generator and an AC/DC/AC IGBT-based PWM converter. The stator winding is connected directly to the 60 Hz grid while the rotor is fed at variable frequency through the AC/DC/AC converter. The DFIG technology allows extracting maximum energy from the wind for low wind speed by optimizing the turbine speed, while minimizing mechanical stresses on the turbine during gusts of wind. In this model the wind speed is maintained constant at 15m/s. The control system uses a torque controller in order to maintain the speed at 1.2 pu. The reactive power produced by the wind turbine is regulated at 0 Mvar. [20].

4.3 Modeling of wind turbine doubly-fed induction generator

The wind turbine and the doubly-fed induction generator are shown in Figure 4.2. The AC/DC/AC converter is divided into two components: the rotor side converter C_{rotor} and the grid-side converter C_{grid}. C_{rotor} and C_{grid} are Voltage-Sourced Converters that use forced-commutated power electronic devices (IGBTs) to synthesize an AC voltage from a DC voltage source. A capacitor connected on the DC side acts as the DC voltage source. A coupling inductor L is used to connect C_{grid} to the grid. The three-phase rotor winding is connected to C_{rotor} by slip rings and brushes and the three-phase stator winding is directly connected to the grid [19], [21].

The power captured by the wind turbine is converted into electrical power by the induction generator and it is transmitted to the grid by the stator and the rotor windings. The control system generates the pitch angle command and the voltage command signals V_r and V_{gc} for C_{rotor} and C_{grid} respectively in order to control the power of the wind turbine, the DC bus voltage and the voltage at the grid terminals. The phase-sequence of the AC voltage generated by C_{rotor} is positive for sub-synchronous speed and negative for super-synchronous speed. The frequency of this voltage is equal to the product of the grid frequency and the absolute value of the slip. C_{rotor} and C_{grid} have the capability for generating or absorbing reactive

power and could be used to control the reactive power or the voltage at the grid terminals [19],[21].

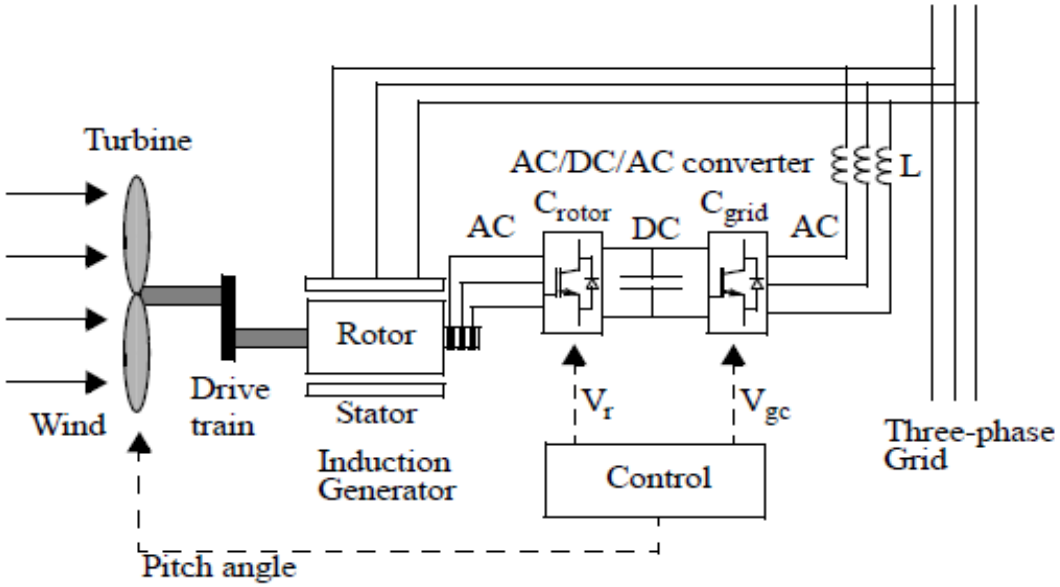

Figure 4.2 the wind turbine and doubly-fed induction generator.

4.3.1 Rotor Side Converter Control system

The rotor side converter is used to control the wind turbine output power and voltage or the output power and reactive power measured at the grid terminals. The power is controlled in order to follow a pre-defined power-speed characteristic named tracking characteristic. This characteristic is illustrated by the ABCD curve in Figure 4.3 superimposed to the mechanical power characteristics of the turbine obtained at different wind speed. The actual speed of the turbine ω_r is measured and the corresponding mechanical power of the tracking characteristic is used as the reference power for the power control loop. The tracking characteristic is defined by four points: A, B, C and D. From zero speed to speed of point A the reference power is zero. Between point A and point B the tracking characteristic is a straight line. Between point B and point C the tracking characteristic is the locus

of the maximum power of the turbine (maxima of the turbine power vs turbine speed curves). The tracking characteristic is a straight line from point C and point D. The power at point D is one per unit (1 p.u.). Beyond point D the reference power is a constant equal to one per unit (1 p.u.).

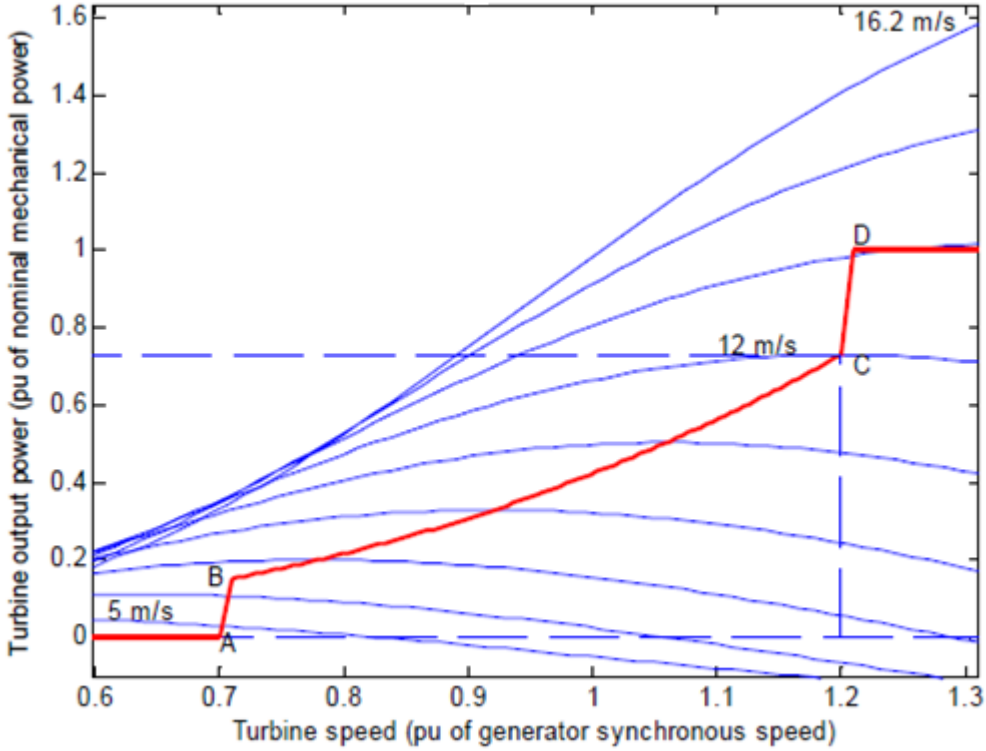

Figure 4.3 Turbine characteristics and tracking characteristic

The generic power control loop illustrated in Figure 4.4. For the rotor-side controller the d-axis of the rotating reference frame used for d-q transformation is aligned with air-gap flux. The actual electrical output power, measured at the grid terminals of the wind turbine, is added to the total power losses (mechanical and electrical) and is compared with the reference power obtained from the tracking characteristic.

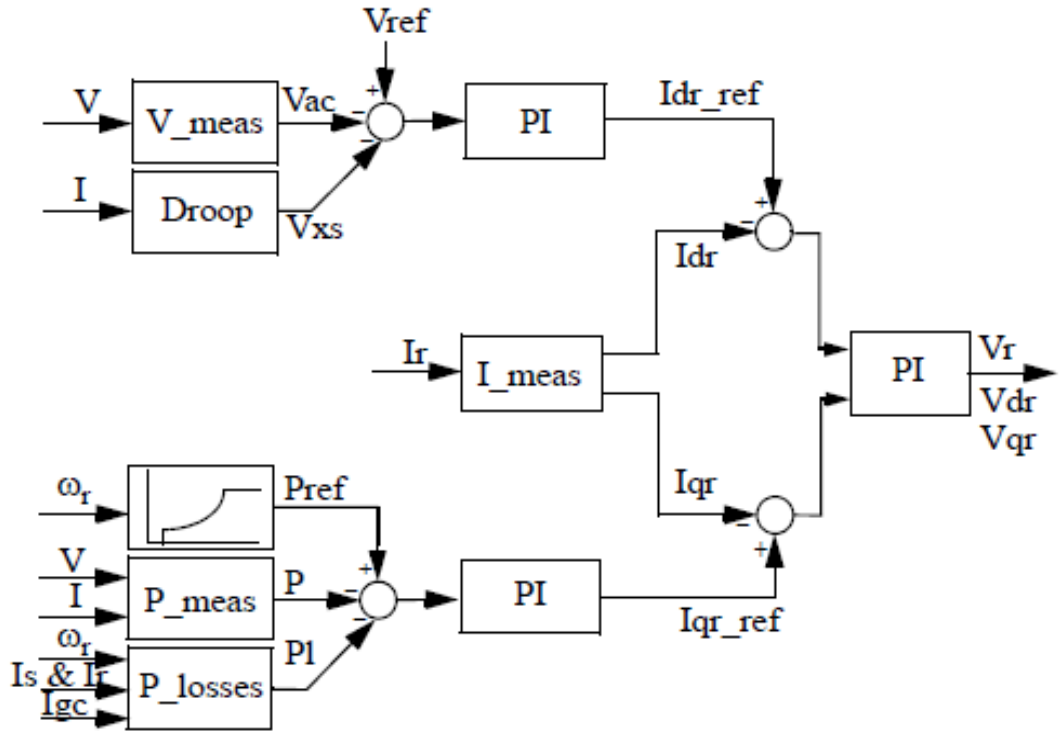

Figure 4.4 rotor-side controller

4.3.2 Grid Side Converter Control system

The grid-side converter is used to regulate the voltage of the DC bus capacitor. For the grid-side controller the d-axis of the rotating reference frame used for d-q transformation is aligned with the positive-sequence of grid voltage. This controller consists of:

- Measurement system measuring the *d* and *q* components of AC current to be controlled as well as the DC voltage V_{dc}.
- An outer regulation loop consisting of a DC voltage regulator. The output of the DC voltage regulator is the reference current *Idgc-ref* for the current regulator (*Idgc* = current in phase with grid voltage which controls active power flow).
- An inner current regulation loop consisting of a current regulator. The current regulatory controls the magnitude and phase of the voltage

generated by converter C $_{grid}$ (*Vgc*) from the *Idgc-ref* produced by the DC voltage regulator and specified *Iq-ref* reference. The current regulator is assisted by feed forward terms which predict the C $_{grid}$ output voltage [19], [21].

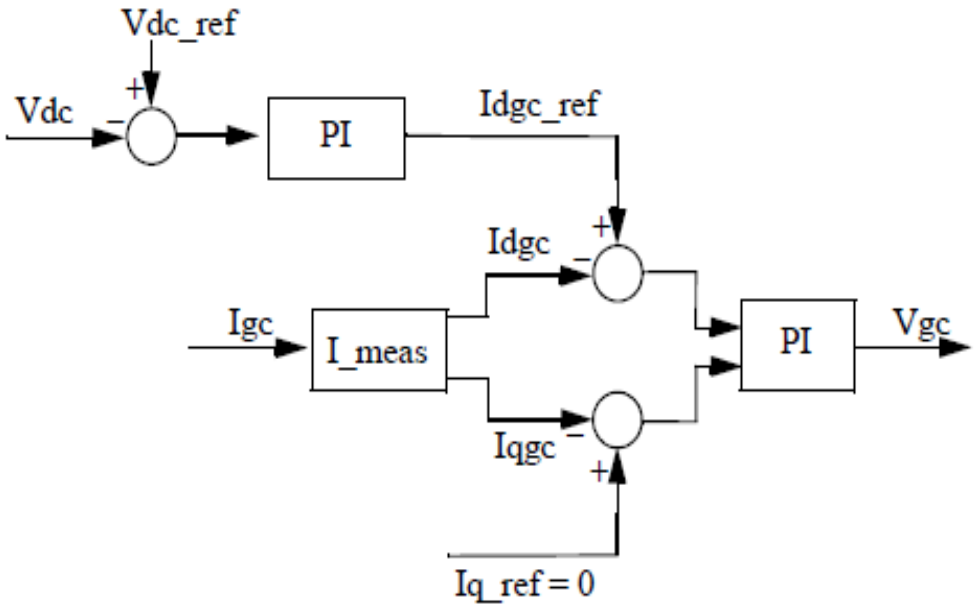

Figure 4.5 Grid-side controllers.

4.4 Simulink Diagram

This is simulink diagram for a doubly-fed induction generator connected to the grid side. The system is connected to a 120 KV, 3-phase source which is connected to a 9 MW wind farm (6 of 1.5 MW each).

The wind-turbine model is a detailed model. The sample time used to discretize the model (Ts=50 microseconds) is specified in the initialization function of the model properties. For a wind speed of 15 m/s, the turbine output power is 1.0 p.u of its rated power, the pitch angle is 8.7 degrees and the generator speed is 1.2 p.u.

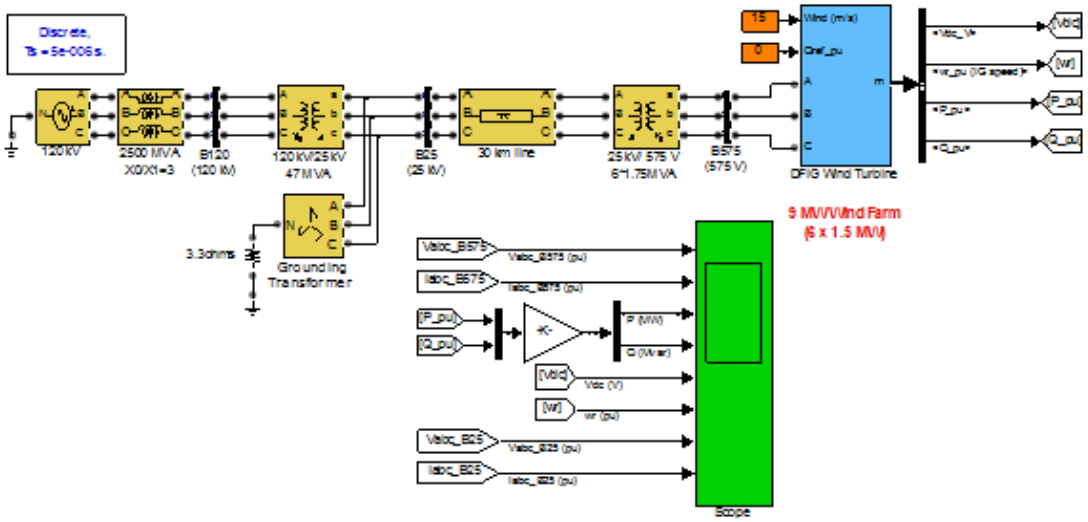

Figure 4.6 Network model schematic.

4.4.1 Generator Data

In the table below implements a model of a variable speed pitch controlled wind turbine using a doubly-fed induction generator (DFIG).

Table 4.1 Generator data.

Number of wind turbines	6
Nominal power	1.5e6 VA
Line to line voltage	575 Vrms
Frequency	60 Hz
Stator resistance	0.023 p.u
Stator inductance	0.18 p.u
Rotor resistance	0.016 p.u
Rotor inductance	0.16 p.u
Magnetizing inductance	2.9 p.u
Inertia constant	0.685 s
Fraction factor	0.01 p.u
Pairs of poles	3

4.4.2 Control Parameters

This is table for control parameters showing different modes of operation in which we can select the voltage regulation mode and Var regulation mode. Here we input the required values of voltage regulator gains (both proportional and integral), power regulator gains, current regulator gains and their respective rate of change.

Table 4.2 Control parameters.

Gains of PI-controller	**K_p**	**K_i**
DC bus voltage regulator	8	400
Grid-side converter current regulator	0.83	5
Rotor-side converter current regulator	0.6	8
Speed regulator	3	0.6
Reactive power(var) and voltage(volt) reulator	0.05	20
Pitch compensation	3	30
Pitch controller	150	-
Frequency of the grid-side PWM carrier	2700 Hz	
Frequency of the rotor-side PWM carrier	1620 Hz	
Maximum pitch angle	27 (deg)	
Maximum rate of change of pitch angle	10 (deg/s)	

4.5 Simulation Results and Discussion

In this model we are observe the steady-state operation of the doubly-fed induction generator and its dynamic response to voltage sag resulting from a remote fault on the 120-KV system.

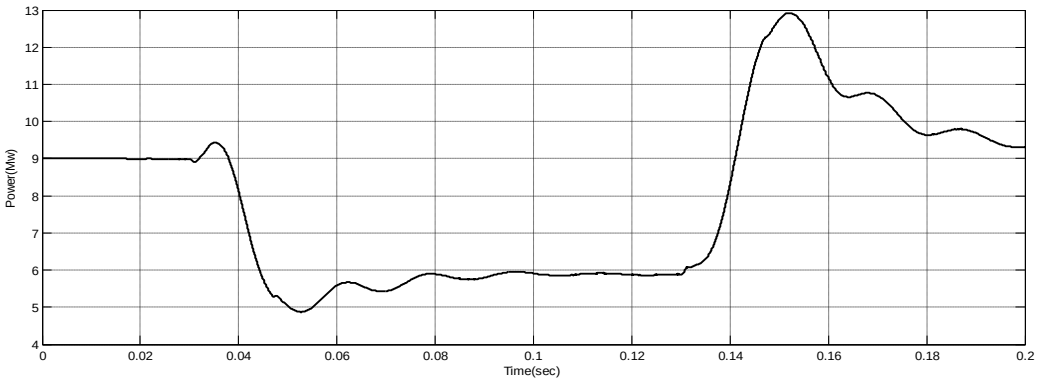

Figure 4.7 Power curve at wind speed 10m/s

Figure 4.7 shows the result of output power when the speed is 10m/s. Initially the power is steady-state and constant in 9 Mw with simple oscillation up to t=0.031 s and at this time the power starting increasing smoothly. As a result of acceleration of the rotor, it is found that the electro motive force decreases and then reduces the torque and thus power value. The power decreases smoothly at t=0.0353s and it is again start increasing at t=0.1301s, due to rotor speed reduction. Also it is found that the maximum power 12.91 Mw at t=0.152s and the minimum power 4.869 Mw at t=0.0526s and the power at t=0.2s is 9.319Mw.

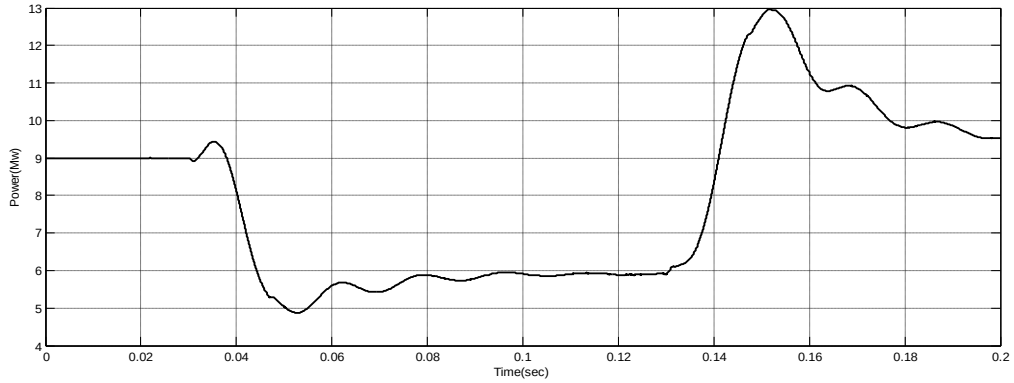

Figure 4.8 Power curve at wind speed 15m/s.

Figure 4.8 shows the result of output power when the speed is 15m/s. Initially the power is steady-state and constant in 9 Mw with simple oscillation up to t=0.031 s and in this time the power starting increasing smoothly. As a result of acceleration of the rotor, it is found that the electro motive force decreases and

then reduces the torque and thus power value. The power decreases smoothly at t=0.0353s and it is again start increasing at t=0.1301s, due to rotor speed reduction. Also it is found that the maximum power 12.96 Mw at t=0.152s and the minimum power 4.87 Mw at t=0.0526s and the power at t=0.2s is 9.528Mw.

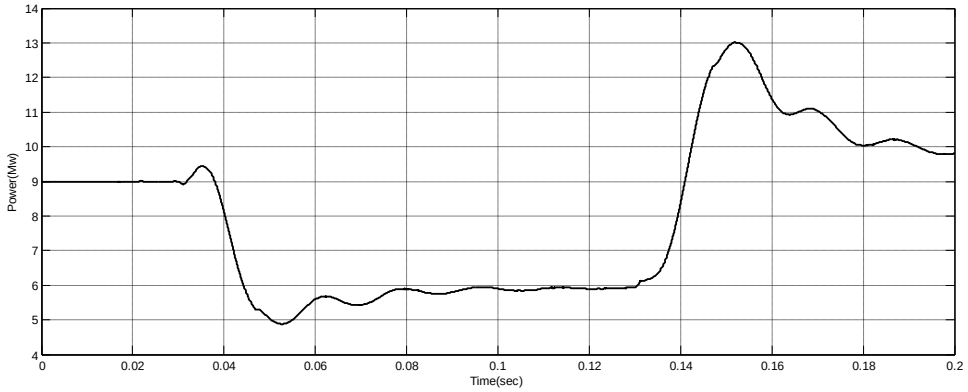

Figure 4.9 Power curve at wind speed 20m/s.

Figure 4.9 shows the result of output power when the speed is 20m/s. Initially the power is steady-state and constant in 9 Mw with simple oscillation up to t=0.031 s and in this time the power starting increasing smoothly. As a result of acceleration of the rotor, it is found that the electro motive force decreases and then reduces the torque and thus power value. The power decreases smoothly at t=0.0353s and it is again start increasing at t=0.1301s, due to rotor speed reduction. Also it is found that the maximum power 13.02 Mw at t=0.152s and the minimum power 4.877 Mw at t=0.0526s and the power at t=0.2s is 9.805Mw.

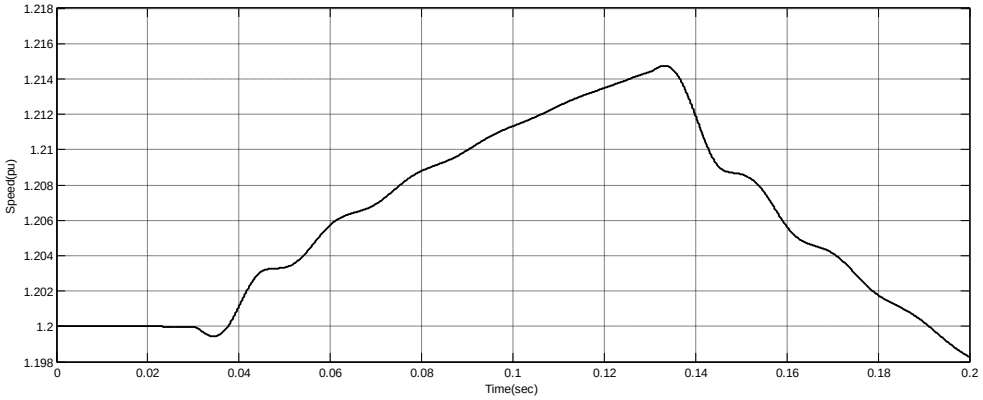

Figure 4.10 Rotor speed curve at wind speed 10m/s

Figure 4.10 shows the result of the rotor speed, when the wind speed is 10m/s. At t=0s the rotor speed is 1.2 pu, power is 9Mw. Due to acceleration of wind the rotor speed increasing smoothly at t=0.0357s and continuous increasing until it reach its maximum, 1.215pu at t=0.134s, after that the rotor speed starting decreases due to operation of control system. At t=0.2s the rotor speed is 1.198pu.

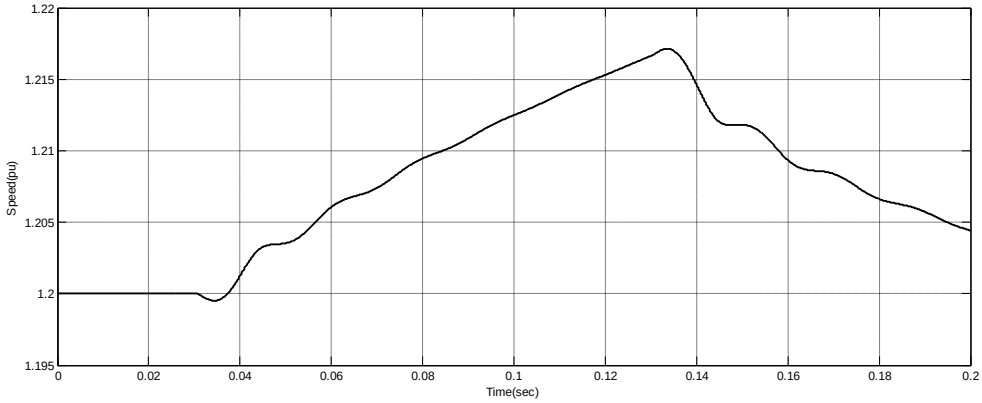

Figure 4.11 Rotor speed curve at wind speed 15m/s

Figure 4.11 shows the result of the rotor speed, when the wind speed is 15m/s. At t=0s the rotor speed is 1.2 pu, power is 9Mw. Due to acceleration of wind the rotor speed increasing smoothly at t=0.0357s and continuous increasing until it reach its maximum, 1.217pu at t=0.134s, after that the rotor speed starting decreases due to operation of control system. At t=0.2s the rotor speed is 1.204pu.

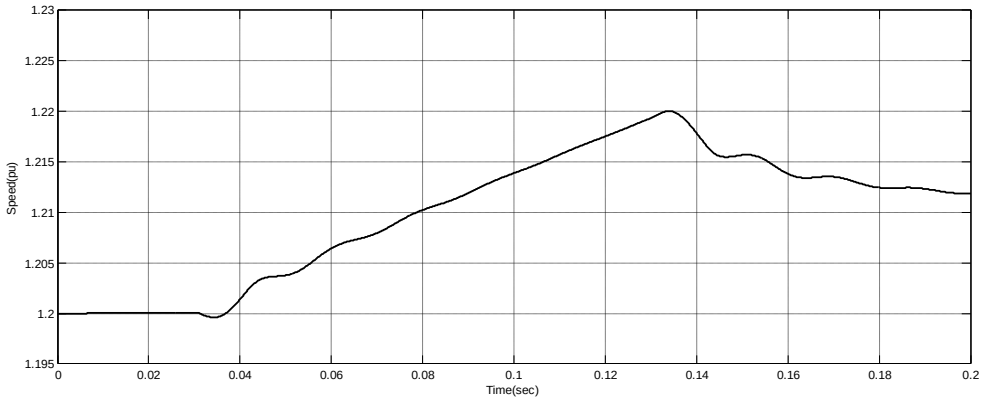

Figure 4.12 Rotor speed curve at wind speed 20m/s

Figure 4.12 shows the result of the rotor speed, when the wind speed is 20m/s. At t=0s the rotor speed is 1.2 pu, power is 9Mw. Due to acceleration of wind the rotor speed increasing smoothly at t=0.0357s and continuous increasing until it reach its maximum, 1.22pu at t=0.134s, after that the rotor speed starting decreases due to operation of control system. At t=0.2s the rotor speed is 1.212pu.

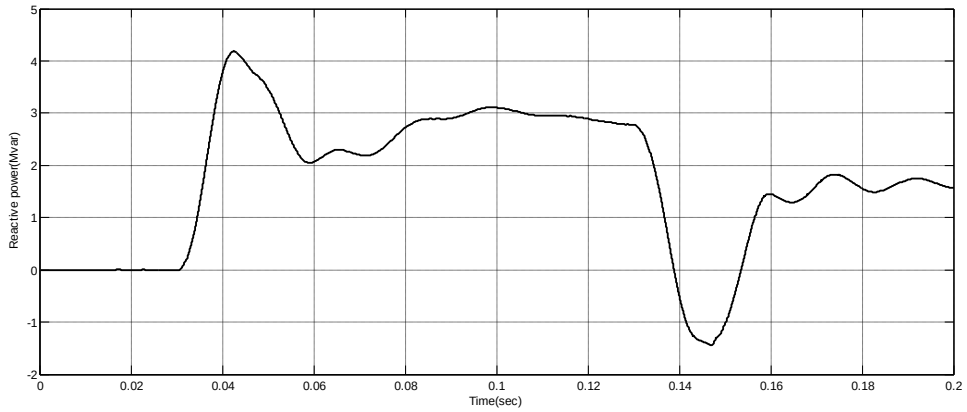

Figure 4.13 Reactive power curve at wind speed 10m/s

Figure 4.13 shows the result of reactive power when the wind speed is 10m/s. Initially the reactive power is constant at 0 Mvar. Due to the active power decreases the reactive power increasing smoothly at t=0.0308s and continuous increasing until it reach its maximum, 4.186Mvar at t=0.042s. Then the reactive power starting decreases because increasing of active power. At t=0.2s the reactive power is 1.565Mvar.

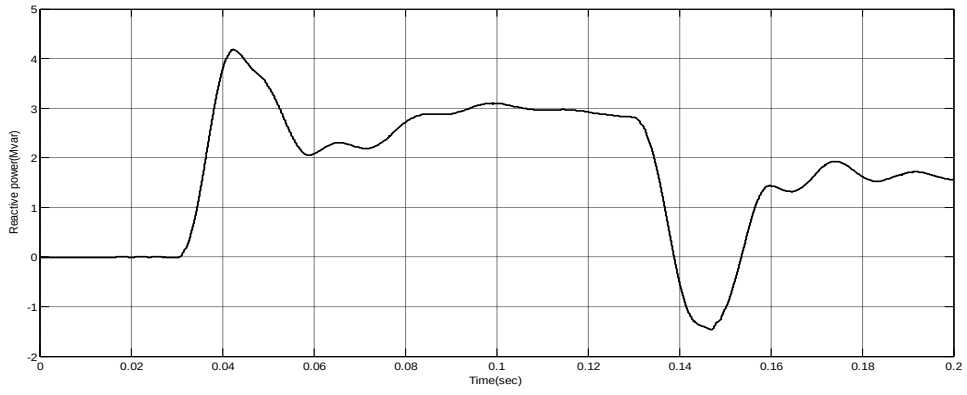

Figure 4.14 Reactive power curve at wind speed 15m/s

Figure 4.14 shows the result of reactive power when the wind speed is 15m/s. Initially the reactive power is constant at 0 Mvar. Due to the active power decreases the reactive power increasing smoothly at t=0.0308s and continuous increasing until it reach its maximum, 4.179Mvar at t=0.0424s. Then the reactive power starting decreases because increasing of active power. At t=0.2s the reactive power is 1.553Mvar.

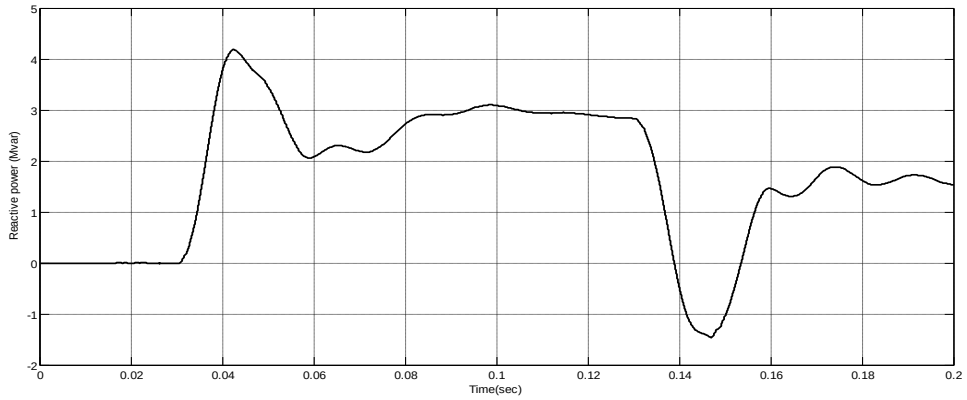

Figure 4.15 Reactive power curve at wind speed 20m/s

Figure 4.15 shows the result of reactive power when the wind speed is 20m/s. Initially the reactive power is constant at 0 Mvar. Due to the active power decreases the reactive power increasing smoothly at t=0.0308s and continuous increasing until it reach its maximum, 4.184Mvar at t=0.0424s. Then the reactive power starting decreases because increasing of active power. At t=0.2s the reactive power is 1.533Mvar.

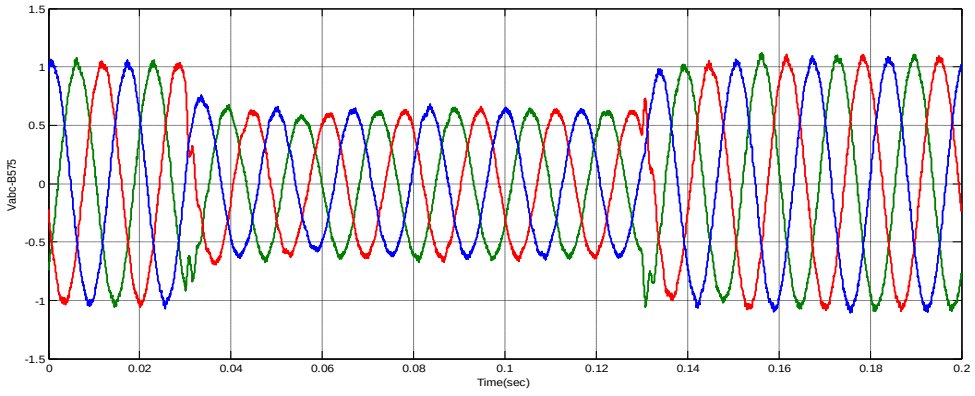

Figure 4.16 Vabc-B575 curves at wind speed 10m/s

Figure 4.16 shows the positive-sequence voltage curves at busbar 575. Initially the doubly-fed induction generator wind farm produces 9 MW. The corresponding turbine speed is 1.2 p.u of generator synchronous speed. And the positive-sequence voltage is 1.0 pu. At t=0.03s the positive-sequence voltage suddenly drops to 0.5 pu until t=0.13s and at this time the voltage returned to 1.0 pu.

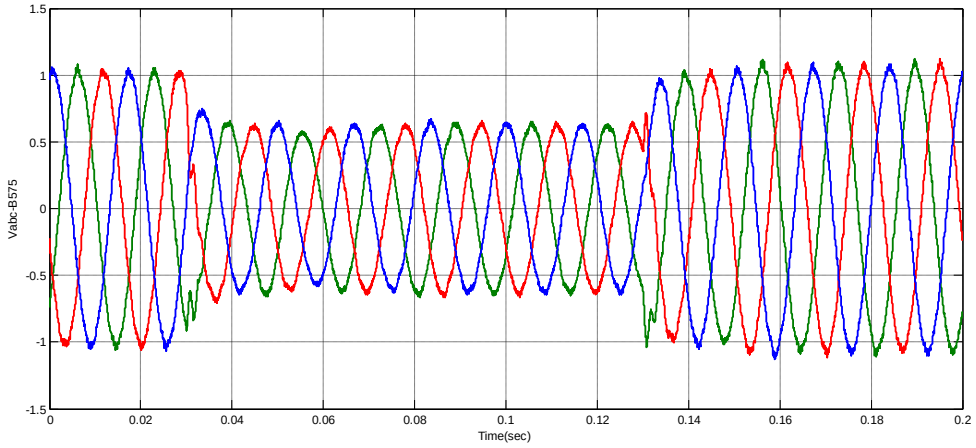

Figure 4.17 Vabc-B575 curves at wind speed 15m/s

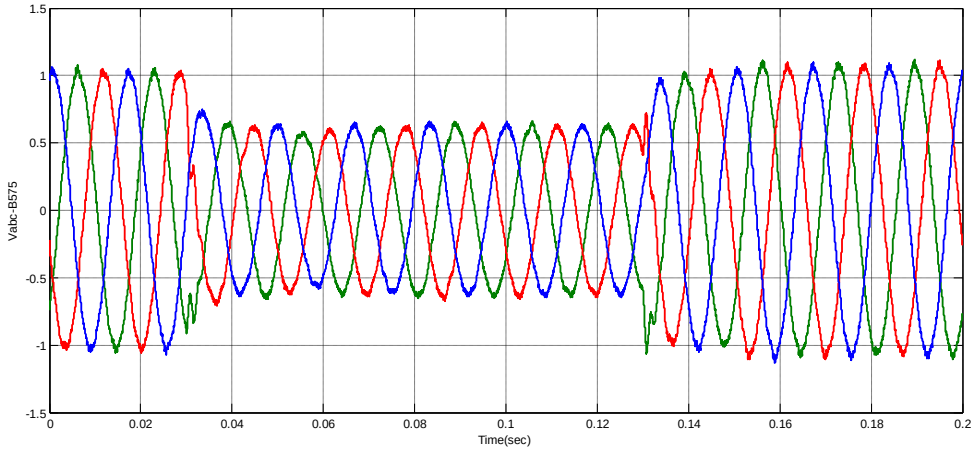

Figure 4.18 Vabc-B575 curves at wind speed 20m/s

Figure 4.17 and 4.18 are shows the positive-sequence voltage curves at busbar 575 at wind speed 15m/s and 20m/s respectively. There are no changes in curves.

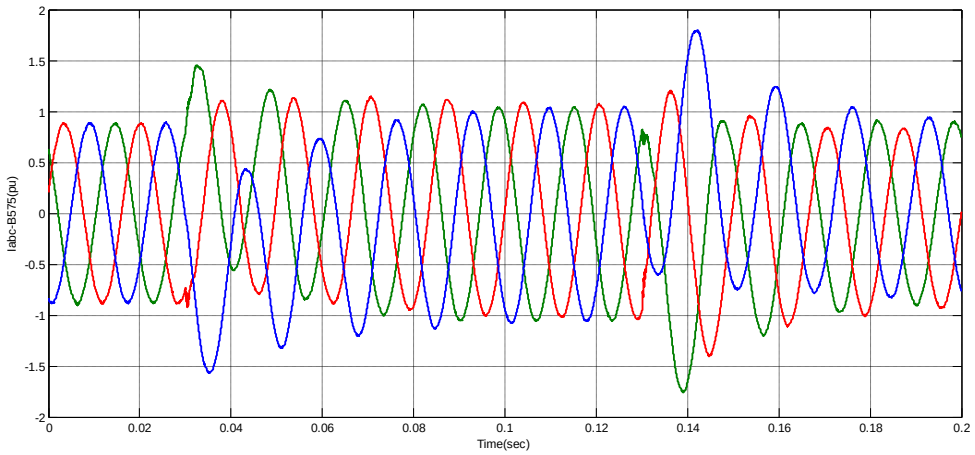

Figure 4.19 Iabc-B575 curves at wind speed 10m/s

Figure 4.19 shows the currents curves in busbar 575 at wind speed 10m/s. Initially the values of currents are 0.8887pu. At t=0.03 the values of current are increasing due to voltage sag up to t=0.13 the values of current are starting decreases.

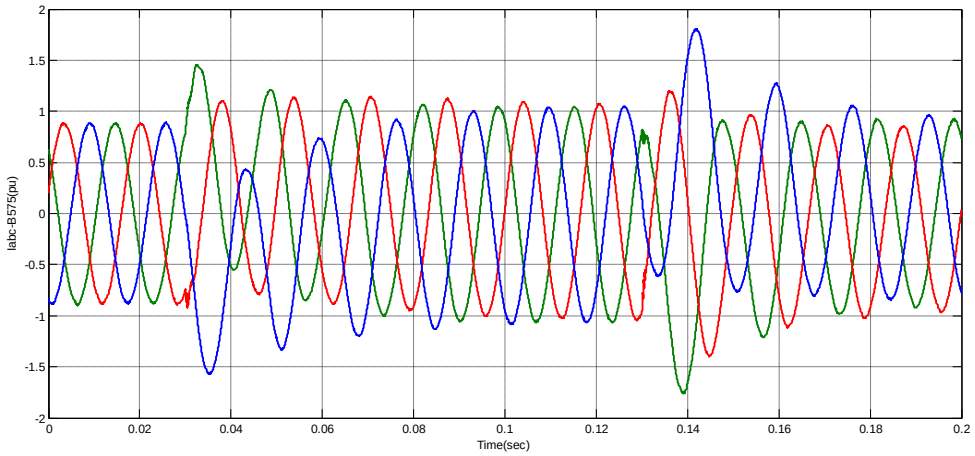

Figure 4.20 Iabc-B575 curves at wind speed 15m/s

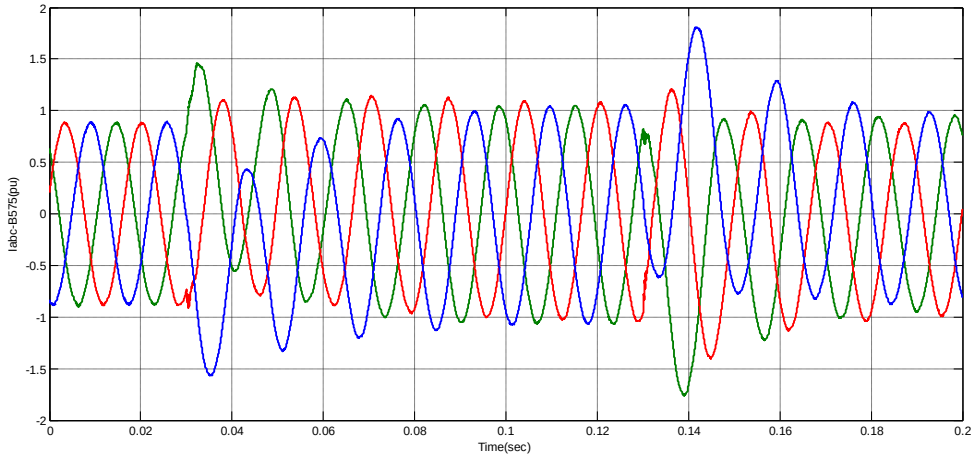

Figure 4.21 Iabc-B575 curves at wind speed 20m/s

Figure 4.20 and 4.21 are shows currents curves in busbar 575 at wind speed 15m/s and 20m/s respectively. There are no changes in curves.

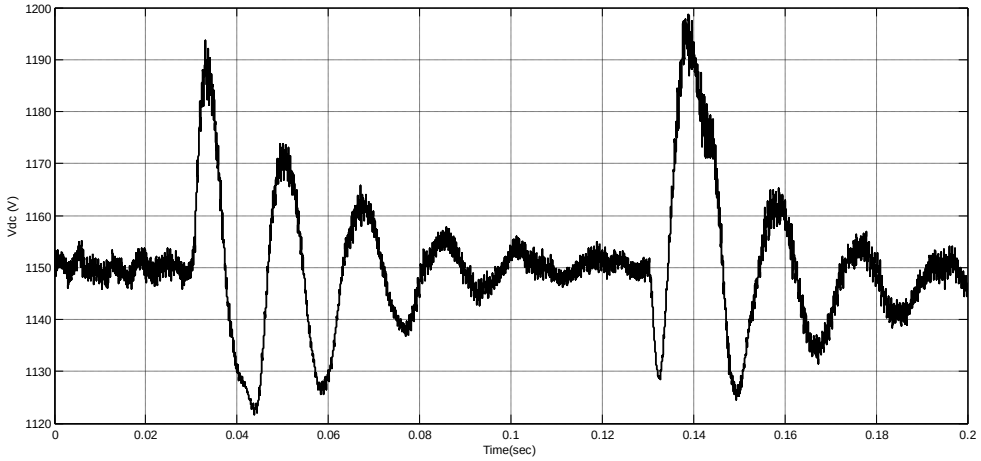

Figure 4.22 DC voltage curve at wind speed 10m/s

Figure 4.24 shows the DC voltage curve at wind speed 10m/s. The DC voltage is regulated at 1150V and reactive power is kept at 0 Mvar. At t=0.03 second the positive-sequence voltage suddenly drops to 0.5 p.u causing an oscillation on the DC bus voltage and on the DFIG output power. During the voltage sag the

control system tries to regulate DC voltage and reactive power at their set points (1150V, 0 Mvar).

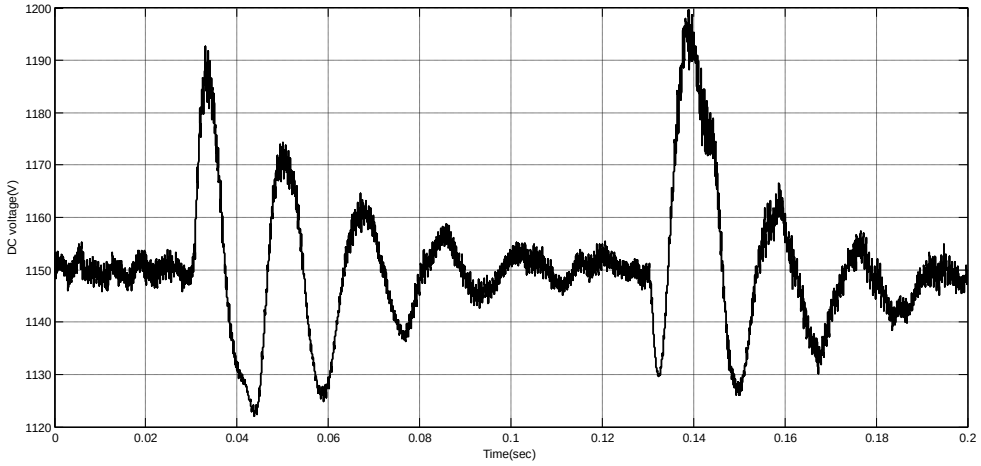

Figure 4.23 DC voltage curve at wind speed 15m/s

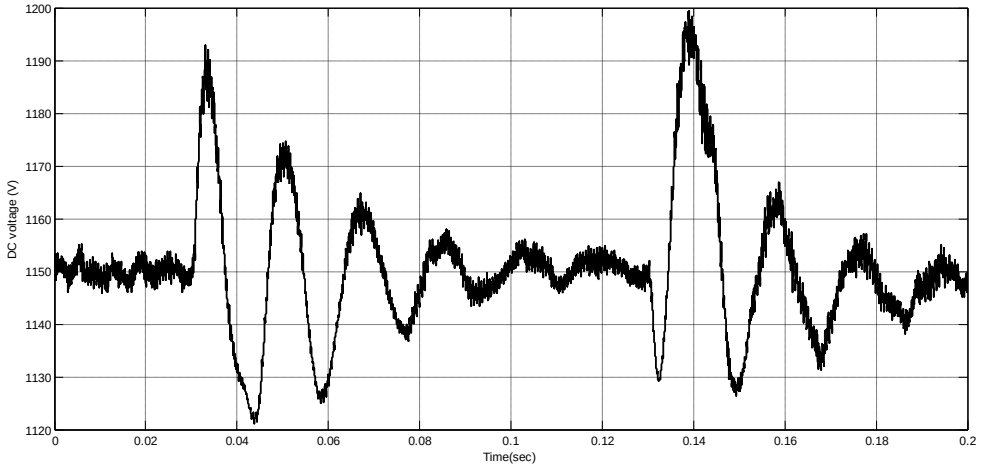

Figure 4.24 DC voltage curve at wind speed 20m/s

Figure 4.23 and 4.24 are shows the DC voltage curve at wind speed 15m/s and 20m/s respectively. There are no changes in curves.

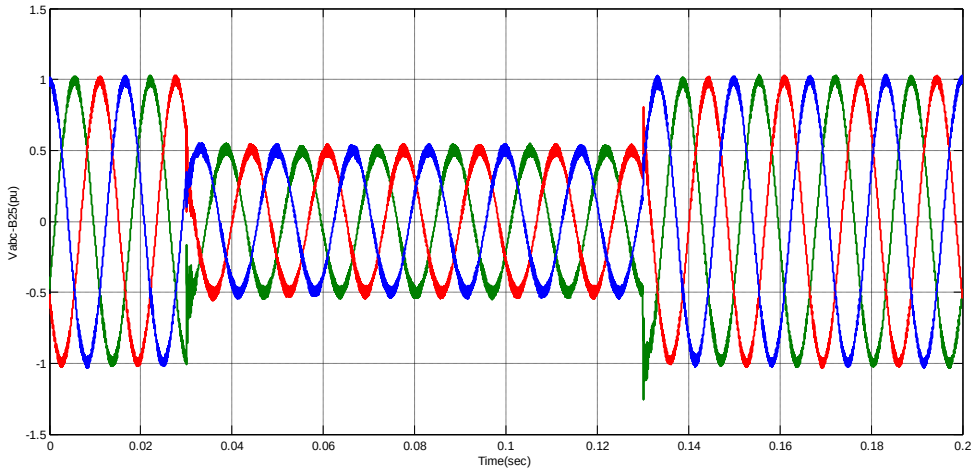

Figure 4.25 Vabc-B25 curves at wind speed 10m/s

Figure 4.25 shows the positive-sequence voltage curves at busbar 25. Initially the positive-sequence voltage is 1.0 pu. At t=0.03s the positive-sequence voltage suddenly drops to 0.5 pu until t=0.13s and at this time the voltage returned to 1.0 pu.

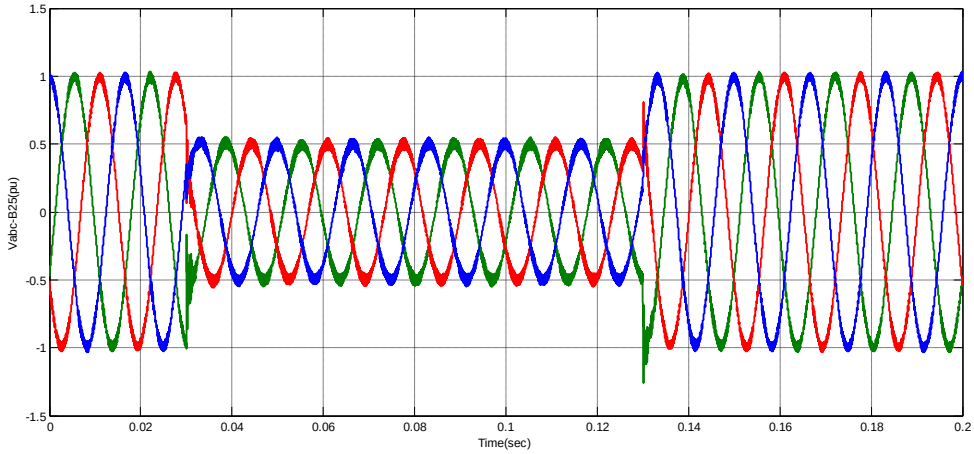

Figure 4.26 Vabc-B25 curves at wind speed 15m/s

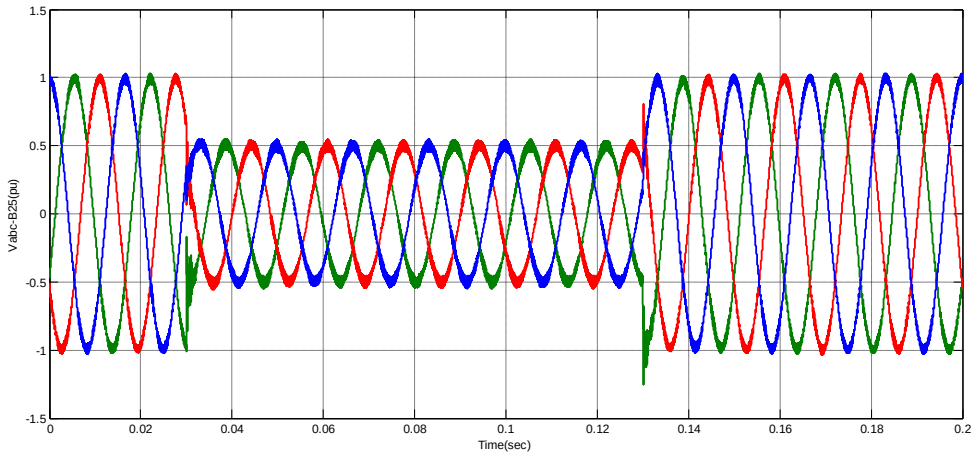

Figure 4.27 Vabc-B25 curves at wind speed 20m/s

Figure 4.26 and 4.27 are shows the positive-sequence voltage curves at busbar 25 at wind speed 15m/s and 20m/s respectively. There are no changes in curves.

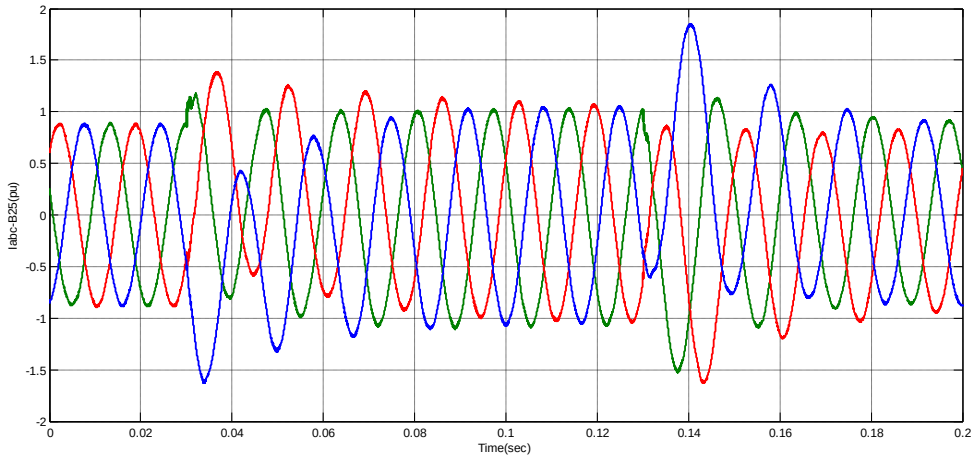

Figure 4.28 Iabc-B25 curves at wind speed 10m/s

Figure 4.30 shows the currents curves in busbar 25 at wind speed 10m/s. Initially the values of currents are 0.8881pu. At t=0.03 the values of current are increasing due to voltage sag up to t=0.13 the values of current are starting decreases.

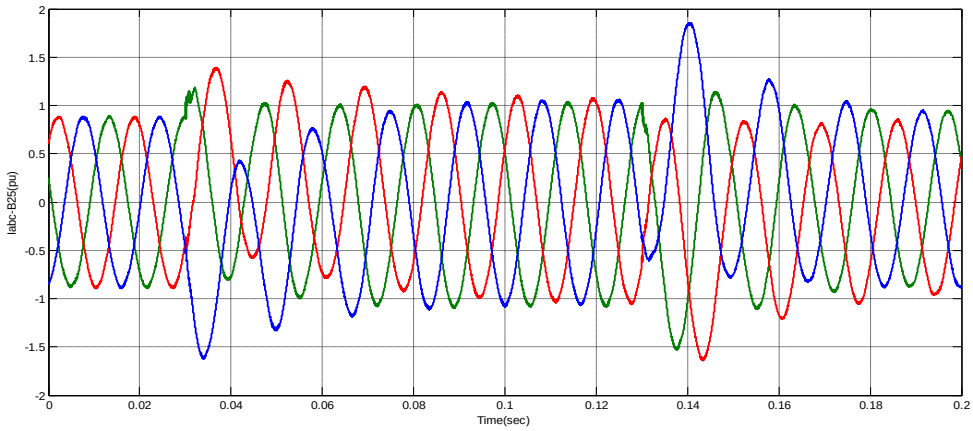

Figure 4.29 Iabc-B25 curves at wind speed 15m/s

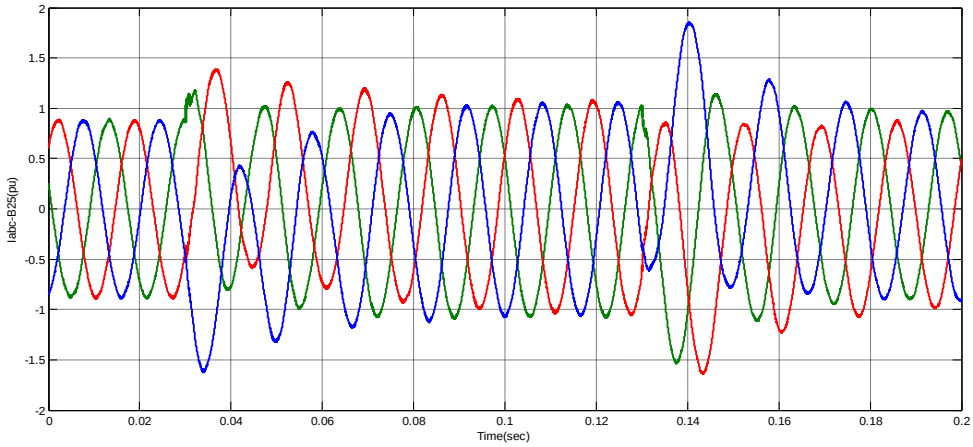

Figure 4.30 Iabc-B25 curves at wind speed 20m/s

Figure 4.20 and 4.30 are shows currents curves in bus-bar 25 at wind speed 15m/s and 20m/s respectively. There are no changes in curves.

4.6 Summary

From the results we are found that if the wind speeds increasing the active power increasing also the maximum rotor speed increasing. The reactive power increasing and then decreases due to the changes in active power. The positive-sequence voltage suddenly drops to 0.5pu then it returned to 1.0pu after 0.1s. The values of currents are changes due to the changes in the voltage. The drops in positive-sequence voltage causing an oscillation on the DC bus-bar voltage and on the DFIG output power.

CHAPTER FIVE
CONCLUSIONS AND RECOMONDATIONS

5.1 Conclusions

The main objective of this dissertation is to give an overview of research and development in the field of modeling and simulation of DFIG coupled with wind turbine. Wind energy conversion system, DFIG equivalent circuit, modeling of different parts and control of DFIG is discussed. So the reader should be familiar with the DFIG Wind Turbine systems. The basic operation of DFIG and it is controls using AC/DC/AC converter have discussed. For best efficiency the DFIG system is used which is connected to grid side and has better control. The rotor side converter (RSC) usually provides active and reactive power control of the machine while the grid side converter (GSC) keeps the voltage of the DC-link constant.

The model is a discrete-time version of the wind turbine doubly-fed induction generator (detailed type) of Matlab-Sim Power system and three values of wind speed were taken. The DFIG is able to provide a considerable contribution to grid voltage support during short circuit periods. Considering the result it can be said that doubly-fed induction generator proved to be more reliable and stable system when connected to grid-side with the proper converter control systems.

The system model of a wind farm 9MW consisting of six 1.5MW wind turbines has been presented. The model has simulated using Matlab/Simulink software. The results of the model illustrated that the maximum extract possible output power from variable wind can be achieved by controlling the back to back convertors systems.

5.2 Recommendations

- In this thesis the response of the doubly-fed induction generator to grid disturbances have been investigated. As always there are many more interesting aspect that can be considered, such as; unsymmetrical voltage dips, voltage harmonics, phase shifts, and frequency dips in the grid voltage.
- Also future work can involve using multi-level STATCOM to reduce the harmonics of the system.
- The transient behaviors of the DFIG-based wind turbine system under disturbances of grid failures should be studied.

REFERENCES

[1] Yi Wang, Lie Xu *"Coordinated Control of DFIG and FSIG-Based Wind Farms under Unbalanced Grid Conditions"* © 2009 IEEE.

[2] F. Poitiers, M. Machmoum, R. Le Doeuff and M.E. Zaim *"Control of A Doubly-Fed Induction Generator For Wind Energy Conversion Systems"* Universite de Nantes, Saint Nazaire, France.

[3] Sarah Foster, Lie Xu *"Coordinated Control and Operation of DFIG and FSIG based Wind Farms"* © 2007 IEEE.

[4] B. Chitti babu, K.B.Mohanty *"Doubly-Fed Induction Generator for Variable Speed Wind Energy Conversion Systems-Modeling & Simulation"* Electrical Engineering Department, National Institute of Technology, Pourkela, INDIA.

[5] Viorica Spoiala, Helga Silaghi and Dragos Spoiala *" Control Of Doubly-Fed Induction Generator System for Wind Turbines"* University of Oradea, Faculty of Electrical Engineering and Information Technology.

[6] Slavomir Seman *"Transient Performance Analysis of Wind-Power Induction Generator"* Doctoral Dissertation.

[7] R. Pena, J.C.Clare, G.M.Asher *"A Doubly fed induction generator using back-to-back PWM converter supplying an isolated load from a variable speed wind turbine"* IEE Prec. Electr. Power Appl. Vol.143, No 5, September 1996.

[8] Markus A. Poller "Doubly-Fed induction Machine Models for Stability Assessment of Wind Farms".

[9] Lie Xu, Dawei Zhi and Barry W. Williams *"Predictive Current Control of Doubly-Fed Induction Generators"* © 2009 IEEE.

[10] ANDREAS PETERSSON *"Analysis, Modeling and Control of Doubly-Fed Induction Generators for Wind Turbine"* ANDREAS PETERSSON, 2005.

[11] Balasubramaniam Babypriya – Rajapalan *"Modeling, Simulation and Analysis of Doubly-Fed Induction Generator For Wind Turbines"* Journal of Electrical Engineering, VOL 60 No. 2, 2009 79-85.

[12] P. S. Mayurappriyan, Jovitha Jerome, M. RamKumar and K. Rajambal *"Dynamic Modeling and Analysis of Wind Turbine Driven Doubly-Fed Induction Generator"* International Journal of RecentnTrends in Engineering Vol. 2 No. 5 November 2009.

[13] Hector A. Pulgar-Painemal, Peter W. Sauer *"Doubly-Fed Induction Machine In Wind Power Generation"* University of Illionis at Urbana- Champaign.

[14] Dawei Zhi, Lie Xu and Barry W. Williams *"Model-Based Predictive Direct power Control of Doubly-Fed Induction Generators"* IEEE transactions on power Electronic, Vol. 25 No. 2 February 2010.

[15] Sarah Foster, Lie Xu and Brendam Fox *"Control of an LCC HVDC System for Connecting Large Offshore Wind Farms with Special Consideration of Grid Fault"* © 2008 IEEE.

[16] Wu Dingguo, Wang Zhixin *"Modeling and Design of Control System for Variable Speed Wind Turbine in All Operation Region"* International Journal of systems application, Engineering & Development issue 3 Volume 1 2007

[17] Azeddine Chaiba, Rachid Abdessemed, Mohamed L. Bendaas *"A TORQUE TRACKING CONTROL ALGORITHM FOR DOUBLY FED INDUCTION GENERATOR"*

[18] A. Dendouga, R. Abdessemed, M. L. Bendaas and Chaiba *"Power Flow Control of a Doubly Fed Induction Generator (DFIG)"* Medwell Journals 2007.

[19] Branislav Dosijanoski *"Simulation of Doubly-Fed Induction Generator in a Wind Turbine"* XI International phD Workshop 17-20 October 2009.

[20] The MathWorks, SimPower Systems For use with Simulink "Wind Turbine Doubly-Fed Induction Generator (Detailed model) help file"

[21] Richard Gagnon, Gilbert Sybille, Serge Bernard, Daniel Pare, Silvano Casoria, Christian Larose *"Modeling and real-Time Simulation of a Doubly-Fed Induction Generator Driven by Wind Turbine"* International conference on power system Transients(IPST05) in motreal, Canada on June 19-23, 2005.